This is a repository copy of *The effect of pre-activation and milling on improving natural clinoptilolite for ion exchange of cesium and strontium*.

White Rose Research Online URL for this paper:
http://eprints.whiterose.ac.uk/144778/

Version: Accepted Version

Article:

Prajitno, MY orcid.org/0000-0002-2944-1470, Harbottle, D orcid.org/0000-0002-0169-517X, Hondow, N orcid.org/0000-0001-9368-2538 et al. (2 more authors) (2020) The effect of pre-activation and milling on improving natural clinoptilolite for ion exchange of cesium and strontium. Journal of Environmental Chemical Engineering, 8 (1). 102991. ISSN 2213-3437

https://doi.org/10.1016/j.jece.2019.102991

Accepted Manuscript

Title: The effect of pre-activation and milling on improving natural clinoptilolite for ion exchange of cesium and strontium

Authors: Muhammad Yusuf Prajitno, David Harbottle, Nicole Hondow, Huagui Zhang, Timothy N. Hunter
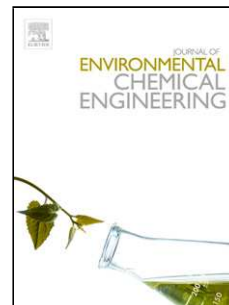
Please cite this article as: Prajitno MY, Harbottle D, Hondow N, Zhang H, Hunter TN, The effect of pre-activation and milling on improving natural clinoptilolite for ion exchange of cesium and strontium, *Journal of Environmental Chemical Engineering* (2019), https://doi.org/10.1016/j.jece.2019.102991

The effect of pre-activation and milling on improving natural clinoptilolite for ion exchange of cesium and strontium

Muhammad Yusuf Prajitno[1*], David Harbottle[1], Nicole Hondow[1], Huagui Zhang[1,2], Timothy N. Hunter[1*]

[1]School of Chemical and Process Engineering, University of Leeds, Leeds, LS2 9JT, U.K.
[2]College of Chemistry and Materials Science, Fujian Province Key Laboratory of Polymer Science, Fujian Normal University, Fuzhou 350007, China
*Corresponding Authors' email: pmmyp@leeds.ac.uk; t.n.hunter@leeds.ac.uk
Phone and Fax: +44 (0)113 343 2790

Graphical abstract
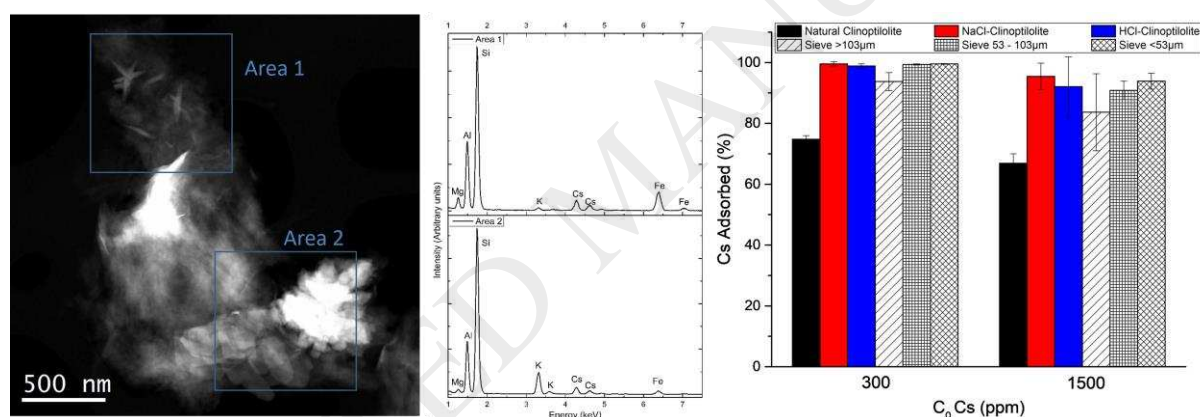
Abstract

Natural clinoptilolite, of relatively low-grade, was investigated for its capability to remove cesium and strontium ions from water and simulated seawater. To improve its capacity, the material was pre-activated with concentrated NaCl and HCl solutions. Additionally, it was milled to a number of < 300 µm size fractions, to expose exchange sites. Electron microscopy was used to characterise the naturally occurring impurities, where regions of high iron and potassium content was shown to correlate to lower levels of cesium adsorption. Adsorption kinetics for natural and activated resins with 5, 300 and 1500 ppm salt solutions were fitted with the Pseudo-Second Order (PSO) rate model. Activation led to clear increases in initial adsorption rate for both Cs^+ and Sr^{2+}, but only enhanced the overall rate constant for Cs^+, due

to the weaker interaction of the Sr^{2+}. Equilibrium isotherms were compared with Langmuir and Freundlich monolayer models, where the adsorption capacity (Q_c) for Cs^+ was 67 mg/g which increased by over 100% with NaCl activation to 140 mg/g. Values for Sr^{2+} were significantly lower at 35 mg/g, with a considerably smaller enhancement with activation to 52 mg/g. Milling of the natural clinoptilolite was found to increase Cs^+ uptake to similar levels as activation, in a linear correlation with specific surface area; although, improvements for Sr^{2+} were again lower, due to its weaker interaction with surface sites. In simulated seawater solutions, all materials gave considerably reduced performance due to K^+ ion competition, with Sr^{2+} uptake decreased more extensively compared to Cs^+. Overall, this work highlights that pre-activation and milling of clinoptilolite can be used to significantly enhance the grade of the ore for nuclear effluent treatment in low-salinity conditions.

1. Introduction

Clinoptilolite is a common ion-exchange media used within the nuclear industry [1], and many research studies have investigated its use to prevent the free release of radionuclides from operational effluents, in particular, cesium and strontium ions [1–26]. Clinoptilolite ores are naturally present in large numbers of deposits around the world, and it does not generally require complicated pre-treatment processes for use, while it has good resistance to radiation exposure [1,16,27]. For example, in the United Kingdom (UK), clinoptilolite is used as an ion-exchange resin for ^{137}Cs and ^{90}Sr removal from nuclear fuel cooling ponds, such as at the Sellafield site in Cumbria [28–32]. The particular materials used in these operations are obtained from a single deposit in California, which has good selectivity for ^{137}Cs and ^{90}Sr, and contains a low level of impurities [28,30–32]. Indeed, while clinoptilolite is relatively abundant, ores with high exchange capacity for both strontium and cesium are far more limited, and there are probable supply issues of nuclear-grade ores for current and future treatment operations worldwide.

Various methods have been used to improve the exchange capacity of natural and synthetic clinoptilolite, as well as many other related materials, for the removal of a number of heavy

metals and radionuclides [18,32–35]. One of the most cost effective pre-treatments, is 'activation' of the ion-exchange sites through the addition of chemicals such as salts or acids in order to get better ion uptake performance [12,18,27,36–38]. Of particular importance for nuclear effluent treatment, which has not been previously studied in detail, is the effect of pre-activation on increasing the uptake of strontium in clinoptilolite, as generally, strontium adsorption capacities are much lower than for cesium [1]. Additionally, it is important to consider the role of pre-activation on adsorption kinetics, as well as equilibrium behaviour. Another technique that may potentially be used to increase natural ion capacity, is to expose additional exchange sites through increasing the surface area to volume ratio by milling [39,40]. While fine milled particles would not be practically used in traditional ion-exchange columns, there has been increasing interest in combining batch adsorption contact tanks with flotation, giving highly efficient uptake and rapid de-watering of nuclear effluents [41–44].

To further understand the extent to which pre-activation and milling can optimise ion-exchange materials, this paper details investigations using relatively low-grade natural clinoptilolite ore, pre-activated with concentrated sodium salt and acid solutions. While clinoptilolite is a well-researched ion-exchange material for a variety of heavy metals, as highlighted, it is vital for applications in nuclear effluent treatment and other related industries, to study the use of natural ores with relatively high levels of impurities, in order to assess the potential for future supply issues. In particular, the use of cheap ion pre-treatments combined with the use of finer milled fractions may provide important engineering solutions to critically expand usable sources for effluent treatments.

To date, there has been no comprehensive study to quantitatively link clinoptilolite contamination to cesium and strontium exchange reduction, which may aid in understanding mechanisms for pre-activation to enhance both the kinetics and equilibrium up-take of these two key radio ions in low-grade ores. Therefore, for this study, characterisation of the zeolite

using elemental mapping from scanning transmission electron microscopy is firstly completed, to indicate naturally occurring contaminants, and their potential impact on adsorption. The influence of activation on both the removal of cesium and strontium are measured, where rate kinetics and equilibrium adsorption behaviour are quantified for various systems. In addition, the performance of various milled sieve fractions are also compared against the un-milled ore. Adsorption reduction in simulated seawater solutions is lastly examined, as clinoptilolite and similar zeolites are known to be significantly affected by high saline effluents [27,30,45,46], which has been a critical issue in the processing of emergency cooling waters at Fukushima, for example [47–49]. Previous studies have highlighted that a number of ions may reduce the exchange process between media and radioactive waste, especially larger monovalent ions such as potassium (K^+) [27,45,50], and it is of interest to examine whether activation mitigates or extenuates these effects.

2. Experimental

2.1. Materials

The natural clinoptilolite used was supplied from Holistic Valley as a $\pm$ 300 µm powder. Cesium chloride (CsCl) and strontium chloride ($SrCl_2$) were Analytical Grade with purity $\geq$ 99.0% and supplied by Sigma-Aldrich and Fisher Scientific, respectively. Meanwhile for the pre-activation, sodium chloride (NaCl) Analytical Grade with purity $\geq$ 99.0% from Fisher Scientific and Hydrochloride Acid (HCl) ACS reagent 37% from Fluka were used. For ion competition, potassium chloride (KCl), sodium chloride (NaCl) and calcium chloride ($CaCl_2$) analytical grade with purity $\geq$ 99.0% were supplied by Fisher Scientific.

It is noted that the sourced clinoptilolite is a relatively low-grade product used as a health supplement. While the grade was not pre-tested specifically, it assumed it was not of a

sufficient grade to be used currently for specific nuclear effluent treatment. However, it is representative of readily available natural ore. Prior to the experiments, the clinoptilolite was rinsed several times with distilled water at neutral pH, with the supernatant being removed in order to get a homogeneous particle size with reduced fines, and to remove any naturally present ions. After every rinse, the supernatant was measured using a conductivity meter until an equilibrium value was reached. The rinsed clinoptilolite was then dried at 100 ºC [1].

2.2. Particle characterisation

The crystal structure of the clinoptilolite was characterised using X-ray diffraction (XRD) with a Bruker D8. Results were analysed using X'Pert HighScore to identify the elemental structure. The zeta potential of clinoptilolite was measured using a Colloidal Dynamics Zeta Probe, in order to determine the change in surface charge between natural and pre-activated clinoptilolite, and through adsorption of different concentrations of cesium and strontium salts.

A Hitachi TM3030 Bench Top scanning electron microscope (SEM) was used to image and analyse the clinoptilolite at low magnification. Further, High Angle Annular Dark Field (HAADF) Scanning Transmission Electron Microscopy (STEM) and Energy Dispersive X-ray (EDX) spectroscopy was used to analyse elements present in the natural clinoptilolite. HAADF-STEM was conducted on an FEI Titan[3] Themis G2 operating at 300 kV fitted with 4 EDX silicon drift detectors, and a Gatan One-View CCD. EDX spectroscopy and mapping was undertaken using the Bruker Esprit v1.9 software. STEM samples were prepared by dispersing the powder in methanol, with a drop placed on a holey carbon coated copper grid. STEM-EDX additionally characterised the location of adsorbed cesium, through measurement of samples mixed with 5000 ppm of cesium chloride for 24 h (using an identical procedure to that outlined in the proceeding section). Samples were then rinsed a number of times to remove excess salt and dried before measurement. Additionally, in order to study the cationic exchange capacity in different pH conditions, 20 g/l dispersions of clinoptilolite were stirred at 300 rpm for 3

hours. The pH changes were measured using a pH meter. 0.1 M of HNO_3 and KOH were used to adjust the pH.

2.3. Salt and acid pre-activation

Clinoptilolite was pre-activated using concentrated sodium chloride salt (denoted 'NaCl-clinopilolite') and hydrochloric acid (denoted 'HCl-clinopilolite'). For NaCl-clinopilolite, 100 g/L solid − liquid ratio of rinsed clinoptilolite was mixed with 1 M NaCl solution at room temperature for 24 h in a rotary carousel. The mixture was then centrifuged, filtered and the suspension rinsed with 300 mL of Milli-Q water, with the washing process repeated several times until conductivity reached an equilibrium value. Figure S1 in the Supplementary Materials presents the conductivity of acid and salt activated samples after a number of washes. The conductivity is observed to reach a baseline, correlating to the natural material, after four washes, which was taken as a minimum for all activation tests. The final suspension was then mixed with 25 mL of methanol for 1 h, before being filtered and dried at 50 ℃ for 3 h [18]. The same overall process was repeated for acid activation, with the use of 1 M HCl in place of the sodium salt [37,38,51].

2.4. Batch adsorption experiments

All the batch adsorption experiments were conducted in polypropylene conical centrifuge tubes in order to prevent Si contamination from glassware and also potential Cs^+ adsorption onto glassware, as evidenced in an earlier study by Chorover et al.[52]. Cesium (Cs^+) and strontium (Sr^{2+}) ion solutions were measured separately to analyse each individually during adsorption experiments.

To measure adsorption kinetics, cesium chloride (CsCl) and strontium chloride ($SrCl_2$) stock solutions (1 M) were diluted with Milli-Q water at neutral pH (which tends to ~6.5, and close to buffered pH values encountered in industry [32]) to a nominal initial concentration of

5 ppm, which is similar to the concentration range used in previous research [1,18], and of relevance for nuclear effluent treatment [18,27]. Then, 0.4 g of clinoptilolite was dispersed in 20 mL samples of the CsCl/SrCl$_2$ solutions, giving a solid/liquid ratio fixed at 20 g/L for different shaking times [12]. Suspensions were placed on an orbital shaker at 150 rpm (at room temperature) for 30 min, 1 h, 2 h, 4 h, 6 h, 12 h, 24 h and 48 h respectively [1]. The dispersions were then centrifuged using a Megafuge 16R for 10 min at 7000 rpm, and the separated supernatants were decanted using a 20 mL syringe with 0.3 µm filter. Natural clinoptilolite dispersions containing higher initial salt levels of 300 ppm and 1500 ppm were also prepared and kinetic concentration differences measured, to understand the effect of initial ion level on dynamic adsorption.

The amount of Cs$^+$ and Sr^{2+} adsorbed by both natural and activated clinoptilolites at each specific time was determined as q_t (mg/g) and removal percent, using the methodologies described in the Appendix (see Eq. A.1-A.2). Adsorption kinetic fits were determined using Pseudo First Order (PFO) and Pseudo Second Order (PSO) rate models to derive the adsorption rate constant (k1 and k2) and initial rate of adsorption (h) (see Appendix Eq. A.3 and Eq. A.4).[1,20,53–58].

To determine the equilibrium adsorption behaviour, both Cs$^+$ and Sr^{2+} from 1 M stock solutions were diluted with Milli-Q water at neutral pH in order to get various initial concentrations from 5 ppm up to 4000 ppm, and again mixed with natural and activated clinoptilolite with a solid/liquid ratio fixed at 20 g/L. All suspensions were then placed on an orbital shaker for 48 h, and supernatants separated as described above. Equilibrium data was fitted with both Langmuir and Freundlich isotherm monolayer adsorption models (see Appendix, Eqs. A.5-A.6).

All supernatants were measured and analysed using an Atomic Absorption Spectrophotometer (AAS) Varian 240fs machine, in which the cesium data were collected using a cesium lamp with wavelength and optimum working range of 459. 3 nm and 5 - 4000 ppm respectively. For strontium, dilutions were required for every Sr^{2+} solution in which the initial concentration was higher than 10 ppm, in order to ensure levels were within the concentration threshold of the AAS. A strontium lamp was used with wavelength and optimum working range set at 460.7 nm and 0.02 - 10 ppm respectively.

2.5. Effect of ion competition on adsorption

To consider the potential impact on cesium and strontium removal in saline conditions, ion competition between K^+, Na^+ and Ca^{2+} ions (as mixed chloride solutions) was analysed, to represent the most significant portion of seawater ions [59]. Cs^+ and Sr^{2+} were firstly fixed at 5 ppm while K^+, Na^+ and Ca^{2+} were fixed at 380 ppm, 10556 ppm and 400 ppm, respectively (as a seawater simulant). Additionally, tests were undertaken with Cs^+ and Sr^{2+} fixed at 5 ppm, while K^+, Na^+ and Ca^{2+} were varied from 5 ppm up to 4000 ppm (with a ratio of 1:1:1) in order to study Cs^+ and Sr^{2+} adsorption in different saline conditions. Sample preparation and analysis with AAS were completed as described above.

2.6. Particle milling and surface area analysis

The effect of particle milling was investigated to study the influence of surface area on the adsorption of cesium and strontium. Clinoptilolite was milled using a PM 100 ball mill at 550 rpm for 20 min [60]. The milled particles were then sieved in different fraction sizes from 103 µm down to less than 53 µm, using a Sieve Shaker AS 200 Control for 10 min. To prove the dispersion homogeneity, all samples were analysed using a Malvern Mastersizer 2000E laser diffractometer, and the particle size distributions of different sieve fractions is shown Figure 1.

Figure 1. insert

This figure indicates that the particle size distribution of natural clinoptilolite is within 180 - 300 μm size range. Additionally, the median d_{50} size of natural clinoptilolite, sieve >103 μm, sieve 53 − 103 μm and sieve <53 μm are 246.04 μm, 120.56 μm, 55.65 μm and 23.15 μm, respectively, with relatively good separation between the fractions. Decreasing the d_{50} from milling should increase the adsorption of ions, because of the greater surface area to volume ratio of each fraction [60–62].

Each of the sieved particle fractions were measured using the Micromeritics Tristar 3000 to determine the Brunauer–Emmett–Teller (BET) surface area. Before active measurements, each sample was degassed using a Micromeritics FlowPrep 060 gradually under N_2 at variable temperatures. The temperature was set at 80°C for 30 min, then increased to 120°C for another 30 min, before finally being degassed at 300°C for 5 h. For the active measurements, the dead volume was initially measured with the He gas as before being removed under vacuum. N_2 gas was then injected and adsorption isotherms recorded, where the amount of adsorbed gas per mass of particle sample is correlated to the total surface area of the particles, assuming monolayer coverage.

The measured surface area of the natural clinoptilolite was 10.812 m^2/g, while the sieve fractions gave 30.949 m^2/g (sieve >103 μm), 42.719 m^2/g (sieve 53 − 103 μm) and 43.606 m^2/g (sieve <53 μm). The surface areas of the acid and salt activated materials were similarly measured, giving 46.521 m^2/g and 47.111 m^2/g for the HCl and NaCl activated respectively. It is noted that an equivalent spherical area for a non-porous particle of 250 μm would be only ~0.01 m^2/g. Hence, the actual specific surface area values (being almost 3 orders of magnitude greater) highlight the influence of the interstitial exchange sites on significantly increasing the material ionic porosity, a critical feature in the ion-exchange performance of zeolites. The increase in BET surface area on activation, also indicates the role of initial charge loading on accessing these porous sites, and gives initial confidence in the success of the activation

processes. Measured surface areas are also broadly consistent with previous work on activated zeolites [24].

3. Results and discussion

3.1. Characterisation of clinoptilolite

Images from the high angle annular dark field (HAADF) scanning transmission electron microscopy (STEM) used to analyse the natural clinoptilolite with adsorbed cesium are shown in Figure 2, with associated elemental mapping. Supplementary Materials Figure S2 displays representative images from SEM analysis at 100x and 1000x magnification, for the natural and activated clinoptilolites. The morphology of the samples are irregular crystals, consistent with crushed natural minerals. There were no changes evident from the pre-activation routine (see Fig. S2).

Figure 2. insert

The energy dispersive X-ray (EDX) spectroscopy analysis shown in Fig. 2, was used to understand both the extent of naturally present surface contamination and its influence on cesium adsorption. In addition to the expected aluminium and silicon peaks (as clinoptilolite is an aluminosilicate zeolite) cesium from adsorption was also detected, as well as several other elements (Fig. 2b-c). EDX spectra from different areas suggested relatively high concentrations of elements such as iron and potassium. Area 1 (Fig. 2d-g) highlighted the presence of iron based contaminants, which also appeared to reduce cesium adsorption, from the low density cesium element map of this area (Fig. 2f). Area 2 suggested additionally, large regions of potassium ions are also present in the natural mineral. This area also had high levels of cesium adsorption, but notably less so in the region of high potassium density. Given that potassium is a strongly competing ion, this is perhaps not surprising, and such adsorbed ionic impurities

could considerably contribute to low adsorption uptake of cesium and strontium [21]. Additionally, mineral impurities (such as those potentially leading to the presence of the iron) may also affect the clinoptilolite performance [1,27].

In order to study the importance of the observed impurities, and also the influence of the sodium and acid activation, XRD patterns of the powder samples were measured and compared to the X'Pert HighScore database, as shown in Supplementary Materials Figure S3. The natural clinoptilolite, as well as both the sodium and acid activated materials, were all matched to calcium type clinoptilolite, with no evidence for a significant presence of other minerals. Such a result would infer that the elemental impurities evident in the STEM-EDX (Fig. 2) are largely from adsorbed surface ionic contaminants, rather than bulk mineral differences. The pre-activation currently does not change the structure of clinoptilolite significantly, but only affects the concentration of exchangeable ions which can increase the surface reactivity [37,63].

The influence of pre-activation on the zeta potential of clinoptilolite is presented in Figure 3, where the potential of the natural clinoptilolite is compared to NaCl-Clinoptilolite and HCl-Clinoptilolite samples. The clinoptilolite is naturally highly negatively charged, which reduces with the activation treatments. These changes indicate that activation not only results in ion-exchange with existing charge groups, but adsorption of sodium and hydrogen ions into interstitial or surface sites with no ions naturally present (thus reducing the net surface negative charge). Such changes are also consistent with the increase in measured specific surface areas on activation. Additionally, the sodium and hydrogen ions will be electrostatically attracted to the negatively charge surface of the clinoptilolite, leading to further adsorption. For highly expandable clays, electrostatic surface interactions can lead to a distinct two layer adsorption model, where firstly, inter-layer ion-exchange sites control interaction, before secondly, surface interactions dominate [44]. While clinoptilolite and zeolites more generally, do not

normally exhibit explicit two site adsorption behaviour, previous studies using other ions, such as lead, have found both monolayer adsorption and heterogeneous surface conditions exist [64].

Figure 3. insert

The influence of electrostatic attraction is also evident from the changes to natural clinoptilolite zeta potential in solutions of increasing cesium and strontium, as shown in Figure 4. Both cesium and strontium adsorption leads to a monotonic decrease in the magnitude of the measured zeta potentials (less negative values) and approach steady-state values, which likely corresponds to the ion adsorption capacity. Again, such changes to zeta potential values indicate that not only ion-exchange, but electrostatic surface adsorption of ions occur. Whether such multiple adsorption site interactions occur through largely homogeneous or heterogeneous exchanges during surface adsorption can be determined from Langmuir and Freundlich fittings (see Section 3.3). However, the monotonic change in zeta potential would also infer there is no direct evidence for a separated dual-site adsorption mechanism, but rather ion-exchange and electrostatic surface adsorption occur collectively. Additionally, the similar magnitudes for the potential changes for both strontium and cesium adsorption would indicate much lower number density of strontium (as it is divalent).

Figure 4. insert

3.2. Adsorption kinetics modelling

The adsorption kinetics of Cs^+ and Sr^{2+} on natural and pre-activated clinoptilolite (NaCl-Clinoptilolite and HCl-Clinoptilolite) are compared for 5 ppm salt solutions in Figure 5 a) and b), where adsorption is shown in terms of q_t (the adsorption ratio, in mg/g) and the percentage removal of the initial 5 ppm ion dose. Additionally, the Cs^+ and Sr^{2+} adsorption kinetics for the natural clinoptilolite at two further initial ion concentrations of 300 ppm and 1500 ppm are shown in the Supplementary Materials (Figure S4). For all cases at 5 ppm presented in Fig. 5,

cesium and strontium ions are observed to reach equilibrium within around 360 min (6 h), which is consistent with previous studies on similar systems [1,18,20,25,65–67]. For the natural clinoptilolite at higher salt levels, equilibrium adsorption occurs at a slightly greater time of 500 min (or ~8 h).

Figure 5. insert

It is noted that in the case of cesium at 5 ppm, the influence of pre-activations does not appear to be significant, in terms of improving adsorption amount (see Fig. 5a). However, this result is likely from the relatively low concentration of cesium used and high removal percentages in all cases, even for the natural non-activated material. It would be expected that for higher cesium dosages, enhancement from activation would become more evident (as discussed in reference to Figure 6a following). Nevertheless, pre-activation does appear to considerably improve adsorbed amounts of strontium (Fig. 5b) with both NaCl and HCl activation similarly enhancing removal from ~60% to almost 100% in the 5 ppm dose [68].

Pseudo-First Order (PFO) and Pseudo-Second Order (PSO) rate analysis (as described within the Appendix, Eq. A.3-A.4) were used to generate equilibrium rate constants and initial adsorption rate values from natural clinoptilolite kinetic adsorption data at 5, 300 and 1500 ppm, as well as the activated clinoptilolites at 5 ppm. The equilibrium rate constant (k_2, g/mg.min) and the initial adsorption rate (h, mg/g.min) derived from the PSO model for all systems are shown in Table 2. The PFO and PSO plots used to fit model values are shown in the Supplementary Materials (Figure S5 and S6) where the R^2 values from PSO values from all experiment were close to 1 and significantly higher than R^2 values from the PFO model. The preference for PSO rate modelling, indicates that the rate-limiting step is the surface chemisorption (PSO), where the removal from a solution is due to physicochemical interactions between the two phases (solid and liquid) [2,20,54,69].

Table 1. insert

Based on results shown in Table 1 for 5 ppm salt concentrations, the pseudo-second order constants (k_2) for Cs^+ are slightly larger through activation with sodium or acid (indicative of the enhanced kinetic interactions) although Sr^{2+} rate constants are not significantly altered (perhaps as ion-surface interaction is weaker in all cases). However, the initial adsorption rate (h) is enhanced considerably for both Cs^+ and Sr^{2+} with clinoptilolite activation. Additionally overall, initial adsorption rate values (mg/g.min) are about twice as large for Cs^+ than with Sr^{2+}, in all cases.

For natural clinoptilolite at the higher initial ion concentrations of 300 and 1500 ppm, there is a distinct drop in the PSO rate constants for both cesium and strontium ions, owing to the increased influence of ion competition on the interaction with adsorption sites, which correlates to the longer times required to reach equilibrium adsorption (see Fig. S4). This behaviour means that adsorption kinetics are more optimal for low initial concentrations of ions, which is consistent with previous work [1,20]. Conversely, the initial adsorption rates (h) increase in a close to linear trend with concentration, owing to the higher initial number density of ions, again in agreement with previous research [1,21,33,55].

3.3. Equilibrium adsorption profiles

The relationship between the equilibrium concentration (C_e) versus final adsorbed amounts of Cs^+ and Sr^{2+} (mg/g clino and adsorbed percentage) are shown in Figure 6 a) and b), respectively. The uptake (q_e) of both ions is increased along with the final concentration (C_e) monotonically as expected for a monolayer coverage [1,18,20,21,70,71]. The percentage of initial ions removed as the equilibrium concentration is increased actually decreases quite considerably with C_e, as all available ion-exchange sites become occupied at relatively low concentrations for both cesium and strontium ion solutions.

Figure 6. insert

It is evident from Fig. 6 that Cs^+ displays much stronger adsorption behaviour compared to Sr^{2+}, with a factor of 2 to 3 in relative adsorbed amount for a given concentration. Such differences compare well to previous literature on cesium and strontium uptake in clinoptilolites and other zeolites [1,10,20,33,72,73]. The reason for the enhanced affinity of the cesium, is the general low energy state of adsorption for large monovalent ions in zeolite ion-exchange sites. The effect of ion valency is significant, where the divalent strontium will be at a higher free energy state than the monovalent cesium [18,74,75]. Additionally on a mass basis (as given) divalent ions have to exchange with two monovalent ions for electron neutrality, and thus total loadings will be lower.

It is also evident that activated clinoptilolite gives pointedly better performance compared to the natural material for both cesium and strontium systems. While differences were not as evident for the 5 ppm kinetic trials (shown in Fig. 4), as the removal percentage was higher in all cases, enhancements in ion exchange capacity are increased with C_e. By initial activation with small monovalent salts such sodium (or acid groups), which are weakly bound compared to other alkali and earth metals, exchange with larger ions including both cesium and strontium are highly energetically favourable [37,76,77]. There is a relatively small difference between salt and acid activated systems, although sodium activation performed best for both cesium and strontium removal overall.

While all reported adsorption tests were completed at neutral pH (correlating with pH values encountered during radionuclide removal in industry [32]), the influence of pH on the cation exchange capacity was correlated by observing changes in pH from H^+ uptake for dispersions at different initial pHs. Given in the Supplementary Materials, Fig. S7 shows the percentage removal of H^+ for systems at initial pHs from $3 - 9$. All systems, apart from pH 9

resulted in removal percentages > 99%, highlighting similar strong cation exchange behaviour over a broad pH range, whereas removal was reduced to < 80% for the pH 9 system, and was negligible for higher pH systems (data not shown). Overall performance is consistent with expectations of a significant reduction in performance for high pH conditions, due to partial degradation of the clinoptilolite [32].

Langmuir and Freundlich theoretical models were applied to the equilibrium adsorption data for both the natural and activated clinoptilolite. The Langmuir model is based on the assumption that each active site of the homogenous surface is occupied by only one molecule, where the energy of adsorption is constant and independent of surface coverage [1,12,21,22,72,78]. Meanwhile, the Freundlich model considers that adsorption takes place on a heterogeneous surface with non-uniform distribution of adsorption energy, which decreases logarithmically with increasing coverage [12,36,64,70,72,79,80]. The results of the Langmuir model fits are presented in Figure 7, in the linear form (where C_e/q_e is plotted against C_e) for a) cesium and b) strontium adsorption. Similarly, the Freundlich fits are presented in Figure 8 (logq_e versus logC_e). Additionally, resulting adsorption coefficients from Cs^+ and Sr^{2+} data are given in Tables 2 and 3, for Langmuir and Freundlich models respectively.

Figure 7. insert

Figure 8. insert

Table 2. insert

Table 3. insert

From Table 3, the adsorption capacity (Q_c) is more than double for cesium adsorption between natural clinoptilolite and NaCl-Clinoptilolite (from ~67 to 140 mg/g). Values for strontium are considerably smaller and show a reduced enhancement with activation (from ~35 to ~52 mg/g). Additionally, activation energies were calculated for cesium and strontium

adsorption on the natural and pre-activated materials using the derived Langmuir constants for the affinity of adsorption (as detailed in the Supplementary Materials, Table S1 and Eq. S1) where energies were higher for Sr^{2+} adsorption, as expected, with significant reductions to both Cs^+ and Sr^{2+} values upon activation. Generally, these results are well within performance requirements for ongoing nuclear effluent treatment, and suggest simple sodium salt pre-activation will enable many lower grade natural clinoptilolite ores to be used in nuclear process plants, greatly expanding the potential supply sites for future procurement.

The Freundlich adsorption affinity constants (K_f, from Table 4) are relatively low in all systems, although again consistent with previous research on cesium removal from clinoptilolite [69]. Proportionally though, activation leads to an even larger increase in performance than for the adsorption capacity (increasing K_f by almost a factor of five in all cases). The low concentration performance assessment from Freundlich fits must be made with some caution however, as R^2 values are lower than for the Langmuir model (although still > 0.9 in most cases). Such differences are similar to trends previously observed, and indicates monolayer coverage of the adsorbent occurs with similar chemical interaction forces across the ion concentration range [1,43,81].

The effect of particle milling on the performance of clinoptilolite was observed by measuring the percentage removal of cesium and strontium salt solutions at initial concentrations of 300 and 1500 ppm. The results are presented in Figure 9, for the natural un-milled material, as well as the salt and acid activated material (also un-milled) in comparison to natural milled particles at three sieve fractions i) < 53 μm, ii) 53-103 μm and iii) > 103 μm mesh.

Figure 9. Insert

It is clear that milling strongly enhances the uptake of cesium, with percentage removal increasing for both initial salt concentrations to around the capacity of the activated materials. Uptake also follows the change in size, with higher removal for smaller sieve fractions, and is in agreement with the understanding that increasing the specific surface area leads to a corresponding increase in adsorption sites, promoting enhanced ion exchange with the cations [60–62]. To quantify the effect of surface area to a greater degree, the adsorption data for the milled fractions was reanalysed, giving the adsorbed percentage for the same initial salt concentrations of 300 and 1500 ppm, in terms of the calculated specific surface areas, for each fraction, as given in Figure 10. Data for the salt activated clinoptilolite is also presented in terms of its associated specific surface area.

Figure 10 insert

It is evident from Figure 10a that, as expected, there is a similar linear increase in adsorbed amount of cesium with the surface area of the clinoptilolite, at both concentrations. Interestingly also, this relationship appears to hold for the activated clinoptilolite, which has a slightly larger surface area than the smallest milled fraction with corresponding increase in adsorption for the 1500 ppm solution (for the 300 ppm solution, both the smallest sieve fraction and activated sample achieve 100% removal). This trend highlights that for cesium, both milling and pre-activation may lead to significant increases in adsorption sites with similar enhancements to material performance.

For strontium adsorption (Figure 10b), the increase in adsorption with surface area of the milled fractions is much less pronounced. Indeed, for the 1500 ppm concentration (which is well beyond concentrations relating to the maximum equilibrium adsorption) almost no increase in capacity is observed until the very highest milled surface area. It is clear also that the effect of pre-activation on adsorption is greater than milling, for equivalent specific surface

areas. As clinoptilolite has interstitial ion-exchange sites, making it ionically porous to some degree, decreasing particle size through milling will lead to an increase in the number of these exposed interstitial sites, as well as the external surface area [82]. However for strontium, the influence of contamination present in the non-activated samples dominates interaction behaviour, and it is clear that milling the material, while increasing the active surface area, does not remove the influence of these contaminants. For example, it appears that the potassium and iron minerals observed with EDX (Fig. 2) may be prevalent throughout the clinoptilolite, and while they will not influence the adsorption of cesium to a high degree (as cesium has higher relative affinity) they appear to continue to disrupt the adsorption of strontium. Thus, the number of available adsorption sites remains low [14,82], and the effect of pre-activation is much more pronounced (as it will lead to the removal of the ionic contaminants, such as the potassium). Therefore, in order to increase the Sr^{2+} adsorption performance, it would be suggested to couple particle milling with salt or acid activation. It is further noted, that the milled clinoptilolite would be too small for a vertical column ion-exchange, as decreasing the particle size will lead to high pressure loss and reduce column performance [70,83,84]. Nevertheless, it would be extremely useful for batch adsorption in a rapid contact mixing tank, where the waste could then be easily dewatered using flotation, for example [41–44,85–87].

3.4. Effect of ion competition on adsorption

The effect of simulated seawater (containing K^+ at 380 ppm, Na^+ at 10556 ppm and Ca^{2+} at 400 ppm) on the adsorption of Cs^+ and Sr^{2+} with natural and pre-activated clinoptilolite is presented in Figure 11. Here, ion removal performance is shown in terms of the distribution coefficient (K_d) as defined in Eq. A.7 within the Appendix.

Figure 11. insert

The influence of salinity on reducing the adsorption of Cs^+ and Sr^{2+} is important for ongoing processing of nuclear effluents from seawater cooling, such as occurring currently at

Fukushima. It is evident from Fig. 11 that the K_d of cesium and strontium from all systems reduces significantly in seawater conditions. Given the relatively low affinity of Na^+ and Ca^{2+} to clinoptilolite [28], it is assumed the major reason for the reduced performance is ion competition from the K^+ ions [1,73]. As potassium is assumed to have a higher affinity than strontium [28], its influence on strontium adsorption in seawater is comparatively greater (with Sr^{2+} distribution coefficients for activated clinoptilolite reducing by two orders of magnitude, in comparison to one order for Cs^+).

To further investigate the reduction of Cs^+ and Sr^{2+} adsorption due to ion competition, distribution coefficients were measured for natural and activated clinoptilolite materials, in solutions of increasing competing ion concentration from 5 up to 4000 ppm (using mixtures of K^+, Na^+ and Ca^{2+} ions in a 1:1:1 ratio) with Cs^+ and Sr^{2+} held at 5 ppm. Results, given in terms of the concentration of competing ions, are shown in Figure 12. Similar to Fig. 11, clear reductions to the distribution coefficient K_d are observed for both cesium and strontium systems, in a power law relationship with competing ion concentration. Indeed, direct measurement of K^+, Na^+ and Ca^{2+} uptake from the saline solution could also be measured simultaneously with the AAS technique, and are reported in the Supplementary Materials, Fig S8. It is observed that ionic affinity follows the expected trend at all solution concentrations of $Cs^+ > K^+ > Sr^{2+} > Na^+ > Ca^{2+}$, and while the general affinity for cesium to clinoptilolite is still above that of potassium [28], the much larger concentration of the latter will dominate surface interactions as the saline solution concentration increases. Interestingly, the exponent gradients for all activated clinoptilolite with cesium and strontium are similar, as interactions are dominated by the competing potassium ions, due to the low 5 ppm level of Cs^+ and Sr^{2+}. Exponents are also higher for the activated clinoptilolite than the natural material, as activation with either sodium or acid will similarly enhance adsorption of potassium, due to its high affinity, and therefore it is apparent that activation by itself cannot reduce salinity effects in

clinoptilolite. Evidence of K^+ dominancy in comparison to Na^+ and Ca^{2+} have also been found in previous research studies [30,45,88,89].

Figure 11. insert

4. Conclusions

This study investigated the use of acid and sodium chloride activation, as well as particle milling, to increase the performance of relatively low-grade clinoptilolite for removing cesium and strontium ions from nuclear effluents. The natural ore was characterised using STEM-EDX and XRD, where regions of high potassium ion contamination and iron based impurities were evident that correlated to areas of lower cesium and strontium uptake. Changes to clinoptilolite zeta potentials with cesium and strontium adsorption indicated heterogeneous surface interactions occurring, driven both by ion-exchange from interstitial sites and electrostatic surface attraction, although there was no evidence of separate two-site adsorption mechanisms.

Adsorption kinetics of natural and pre-activated materials in 5 ppm Cs^+ and Sr^{2+} salts were fitted using a Pseudo-Second Order model with the average linear regression (R^2) ~ 0.99 in all cases. While activation increased the initial adsorption rate of both cesium and strontium, the overall rate constant (k_2) was only enhanced in cesium systems, due to the general low affinity of the strontium. Equilibrium isotherms were compared with Langmuir and Freundlich monolayer models, with the former providing closer fits. The Langmuir adsorption capacity (Q_c) for cesium was increased by over 100% in sodium activated clinoptilolite (from ~67 to 140 mg/g), while values for strontium were considerably smaller with a lower enhancement with activation of ~50% (from ~35 to ~52 mg/g).

Additionally, the effect of milling was observed to give a similar increase in performance to activation for cesium removal, with a strong linear dependency between adsorbed amount and overall specific surface area, where a combination of these two techniques will likely to

lead to a much greater ion-exchange capacity. The influence of contaminants on strontium removal in milled fractions was notably more significant, which reduced relative adsorption in comparison to associated surface area increases on un-activated samples. The influence of ion competition on adsorption was also investigated, using solution mixtures of Na^+, Ca^{2+} and K^+, to represent seawater type solutions. The distribution coefficients (k_d) of both cesium and strontium were significantly reduced, with the magnitude of reduction directly proportional to the concentration of competing ions (from power-law fits) while pre-activation actually led to a more critical drop-off in uptake. Collectively, these results highlight that pre-activation and milling could be used to considerably extend the range of natural clinoptilolite ores suitable for nuclear treatment processing of relatively fresh water effluents, but for high saline waters, modern synthetic products will still be required.

Acknowledgments

APPENDIX

The amount of Cs^+ and Sr^{2+} adsorbed by natural and activated clinoptilolite in kinetics experiments, was determined at each specific time as q_t (mg/g) obtained from Equation A.1. Here, C_o (ppm) is the initial concentration of salt ion, C_e (ppm) is final equilibrium concentration, m (g) is the mass of adsorbent and V (l) is the volume of the suspension.

$$q_t = \frac{(C_0 - C_e)}{m}V \qquad (A.1)$$

The percent adsorption of Cs^+ and Sr^{2+} was determined using Equation A.2, where, C_o (ppm) and C_e (ppm) are as defined above.

$$\% = \frac{(C_0 - C_e)}{C_0} \times 100\%$$ (A.2)

The adsorption kinetics were analysed with Pseudo-First Order (PFO) and Pseudo-Second Order (PSO) rate models, as given in Equation A.3 and Equation A.4, respectively [18,20,53,54]. Here, q_t and q_e (mg/g) represent the amount of solute adsorbed per gram of sorbent at any time and at equilibrium respectively, k_2 (g/mg.min) is the observed rate constant of the PSO model and t is time.

$$\frac{d_q}{d_t} = k_1(q_e - q_t)$$ (A.3)

Note, normally the initial adsorption rate is also used for comparison, h (mg/g.min), where **h = k$_2$q$_e$^{2}**.

$$\frac{t}{q_t} = \frac{1}{k_2 q_e{}^2} + \frac{1}{q_e}t$$ (A.4)

Many models have been developed to represent various types of adsorption processes, where Langmuir and Freundlich models are probably the most frequently used for monolayer adsorption [12,18,72,73]. The Langmuir model assumes that the solid surfaces have uniform sites, and no interaction between sorbed ions takes place, and thus all adsorbed species interact only with adsorption sites [37]. The isotherm can be expressed in the linear form, as shown in Equation A.5.

$$\frac{C_e}{q_e} = \frac{1}{Q_c b} + \frac{1}{Q_c}.C_e$$ (A.5)

Here, q_e (mg/g) and C_e (ppm) denote the equilibrium concentration of sorbate in the solid and the liquid phase, Q_c(mg/g) is the maximum adsorption capacity and b (dm^3/g) is the

Langmuir constant related to the energy of adsorption. A linear relationship can be obtained by plotting $\frac{C_e}{q_e}$ against C_e.

Alternatively, the empirical Freundlich model assumes an energetically heterogeneous set of sorption sites with the sorption energy varying exponentially [27]. The linear form of this isotherm model is given by Equation A.6.

$$\log q_e = \log K_f + \frac{1}{n}\log C_e \qquad (A.6)$$

Here, q_e (mg/g) and C_e (ppm) are as defined throughout, while and K_f (mg/g) is the adsorption affinity constant, which effectively gives the low concentration threshold adsorption value. The proportional fitting constant n quantifies performance changes with concentration variance, and is again dependent on the energy of adsorption.

The amount of solute adsorbed in reference to the initial solution concentration, can be represented by the distribution coefficient, K_d (ml/g), as shown in Equation A.7 [27,90], where all symbols are as previously defined.

$$K_d = \frac{C_o - C_e}{C_e}\frac{V}{m} \qquad (A.7)$$

References

[1]   I. Smičiklas, S. Dimović, I. Plećaš, Removal of Cs1+, Sr2+ and Co2+ from aqueous solutions by adsorption on natural clinoptilolite, Appl. Clay Sci. 35 (2007) 139–144.

[2]   L.L. Ames Jr, Effect of base cation on the cesium kinetics of clinoptilolite, General Electric Co. Hanford Atomic Products Operation, Richland, Wash., 1962.

[3]   J.H. Koon, W.J. Kaufman, Optimization of ammonia removal by ion exchange using clinoptilolite, (1971).

[4]   S.E. Jorgensen, O. Libor, K. Lea Graber, K. Barkacs, Ammonia removal by use of clinoptilolite, Water Res. 10 (1976) 213–224.

[5]   K. Koyama, Y. Takeuchi, Clinoptilolite: The distribution of potassium atoms and its role in thermal stability, Zeitschrift Fur Krist. - New Cryst. Struct. 145 (1977) 216–239.

[6]   E. Valcke, B. Engels, A. Cremers, The use of zeolites as amendments in radiocaesium- and radiostrium-contaminated soils: A soil-chemical approach. Part I: Cs-K exchange in clioptilolite and mordenite., Zeolites. 18 (1997) 205–211.

[7]   E. Valcke, B. Engels, A. Cremers, The use of zeolites as amendments in radiocaesium- and radiostrontium-contaminated soils: A soil-chemical approach. Part II: Sr-Ca exchange in clinoptilolite, mordenite, and zeolite A, Zeolites. 18 (1997) 212–217.

[8]   P. Rajec, F. Macášek, M. Féder, P. Misaelides, E. Šamajová, Sorption of caesium and strontium on clinoptilolite-and mordenite-containing sedimentary rocks, J. Radioanal. Nucl. Chem. 229 (1998) 49–55.

[9]   H. Faghihian, M. Ghannadi Marageh, H. Kazemian, The use of clinoptilolite and its sodium form for removal of radioactive cesium, and strontium from nuclear wastewater and Pb2+ Ni2+ Cd2+ Ba2+ from municipal wastewater, Appl. Radiat. Isot. 50 (1999) 655–660.

[10]   R.M. Woods, M.E. Gunter, Na-and Cs-exchange in a clinoptilolite-rich rock: Analysis of the outgoing cations in solution, Am. Mineral. 86 (2001) 424–430.

[11]   M.V. Mier, R.L. Callejas, R. Gehr, B.E.J. Cisneros, P.J.J. Alvarez, Heavy metal removal with mexican clinoptilolite:: multi-component ionic exchange, Water Res. 35 (2001) 373–378.

[12]   A. Abusafa, H. Yücel, Removal of 137Cs from aqueous solutions using different cationic forms of a natural zeolite: Clinoptilolite, Sep. Purif. Technol. 28 (2002) 103–116.

[13]   R. Petrus, J. Warchoł, Ion exchange equilibria between clinoptilolite and aqueous solutions of Na+/Cu 2+, Na+/Cd 2+ and Na+/Pb 2+, Microporous Mesoporous Mater. 61 (2003) 137–146.

[14]   R. Leyva-Ramos, G. Aguilar-Armenta, L. V Gonzalez-Gutierrez, R.M. Guerrero-Coronado, J. Mendoza-Barron, Ammonia exchange on clinoptilolite from mineral deposits located in Mexico, J. Chem. Technol. Biotechnol. 79 (2004) 651–657.

[15]   M. Çulfaz, M. Yağız, Ion exchange properties of natural clinoptilolite: lead–sodium and cadmium–sodium equilibria, Sep. Purif. Technol. 37 (2004) 93–105.

[16] P. Rajec, K. Domianová, Cesium exchange reaction on natural and modified clinoptilolite zeolites, J. Radioanal. Nucl. Chem. 275 (2007) 503–508.

[17] D. Moraetis, G.E. Christidis, V. Perdikatsis, Ion exchange equilibrium and structural changes in clinoptilolite irradiated with β-and γ-radiation: Monovalent cations, Am. Mineral. 92 (2007) 1714–1730.

[18] E.H. Borai, R. Harjula, L. malinen, A. Paajanen, Efficient removal of cesium from low-level radioactive liquid waste using natural and impregnated zeolite minerals, J. Hazard. Mater. 172 (2009) 416–422.

[19] M.S.-R. E. Xingu-Contreras, G. García-Rosales, I. García-Sosa, A. Cabral-Prieto, Characterization of natural zeolite clinoptilolite for sorption of contaminants, Hyperfine Interact. (2015) 1–12.

[20] D.A. De Haro-Del Rio, S. Al-Joubori, O. Kontogiannis, D. Papadatos-Gigantes, O. Ajayi, C. Li, S.M. Holmes, The removal of caesium ions using supported clinoptilolite, J. Hazard. Mater. 289 (2015) 1–8.

[21] S. Amanipour, H. Faghihian, Potassium hexacyanoferrate–clinoptilolite adsorbent for removal of Cs+ and Sr2+ from aqueous solutions, Int. J. Environ. Stud. 74 (2017) 86–104.

[22] R. Petrus, J.K. Warchoł, Heavy metal removal by clinoptilolite. An equilibrium study in multi-component systems, Water Res. 39 (2005) 819–830.

[23] R. Cortés-Martínez, M.T. Olguín, M. Solache-Ríos, Cesium sorption by clinoptilolite-rich tuffs in batch and fixed-bed systems, Desalination. 258 (2010) 164–170.

[24] N. Mansouri, N. Rikhtegar, H.A. Panahi, F. Atabi, B.K. Shahraki, Porosity, characterization and structural properties of natural zeolite - clinoptilolite - As a Sorbent, Environ. Prot. Eng. 39 (2013) 139–152.

[25] I. Rodríguez-Iznaga, V. Petranovskii, G. Rodríguez-Fuentes, Ion-exchange of amino- and aqua-complexes of nickel and cobalt in natural clinoptilolite, J. Environ. Chem. Eng. 2 (2014) 1221–1227.

[26] L. Yosefi, M. Haghighi, S. Allahyari, S. Ashkriz, The beneficial use of HCl-activated natural zeolite in ultrasound assisted synthesis of Cu/clinoptilolite--CeO2 nanocatalyst used for catalytic oxidation of diluted toluene in air at low temperature, J. Chem. Technol. Biotechnol. 90 (2015) 765–774.

[27] H. Mimura, K. Akiba, Adsorption Behavior of Cesium and Strontium on Synthetic Zeolite P, J. Nucl. Sci. Technol. 30 (1993) 436–443.

[28] A. Dyer, Use of zeolites in the treatment of nuclear waste, in: Anal. Proc., 1993: pp. 190–191.

[29] S. Owens, M. Higgins-Bos, M. Bankhead, J. Austin, Using chemical and process modelling to design, understand and improve an effluent treatment plant, Also This Issue. (2015) 4.

[30] S. Handley-Sidhu, T.K. Mullan, Q. Grail, M. Albadarneh, T. Ohnuki, L.E. Macaskie, Influence of pH, competing ions, and salinity on the sorption of strontium and cobalt onto biogenic hydroxyapatite., Sci. Rep. 6 (2016) 23361.

[31] A. Dyer, T.I. Emms, Cation exchange in high silica zeolites, J. Mater. Chem. 15 (2005) 5012–5021.

[32] A. Dyer, J. Hriljac, N. Evans, I. Stokes, P. Rand, S. Kellet, R. Harjula, T. Moller, Z. Maher, R. Heatlie-Branson, J. Austin, S. Williamson-Owens, M. Higgins-Bos, K. Smith, L. O'Brien, N. Smith, N. Bryan, The use of columns of the zeolite clinoptilolite in the remediation of aqueous nuclear waste streams, J. Radioanal. Nucl. Chem. 318 (2018) 2473–2491.

[33] H. Faghihian, M. Iravani, M. Moayed, Application of PAN-NaY Composite for CS+ and SR2+ Adsorption: Kinetic and Thermodynamic Studies, Environ. Prog. Sustain. Energy. 34 (2015) 999–1008.

[34] K.Z. Elwakeel, A.A. Atia, E. Guibal, Fast removal of uranium from aqueous solutions using tetraethylenepentamine modified magnetic chitosan resin, Bioresour. Technol. 160 (2014) 107–114.

[35] K.Z. Elwakeel, H.A. El-Sadik, A.S. Abdel-Razek, M.S. Beheary, Environmental remediation of thorium(IV) from aqueous medium onto Cellulosimicrobium cellulans isolated from radioactive wastewater, Desalin. Water Treat. 46 (2012) 1–9.

[36] L.M. Camacho, R.R. Parra, S. Deng, Arsenic removal from groundwater by MnO2-modified natural clinoptilolite zeolite: Effects of pH and initial feed concentration, J. Hazard. Mater. 189 (2011) 286–293.

[37] M.M. Motsa, B.B. Mamba, J.M. Thwala, T.A.M. Msagati, Preparation, characterization, and application of polypropylene-clinoptilolite composites for the selective adsorption of lead from aqueous media, J. Colloid Interface Sci. 359 (2011) 210–219.

[38] B.B. Mamba, D.W. Nyembe, A.F. Mulaba-Bafubiandi, The effect of conditioning with NaCl, KCl and HCl on the performance of natural clinoptilolite's removal efficiency of Cu2+ and Co2+ from Co/Cu synthetic solutions, Water SA. 36 (2010) 437–444.

[39] A. Djukić, U. Jovanović, T. Tuvić, V. Andrić, J.G. Novaković, N. Ivanović, L. Matović, The potential of ball-milled Serbian natural clay for removal of heavy metal contaminants from wastewaters: Simultaneous sorption of Ni, Cr, Cd and Pb ions, Ceram. Int. 39 (2013) 7173–7178.

[40] M. Vhahangwele, G.W. Mugera, The potential of ball-milled South African bentonite clay for attenuation of heavy metals from acidic wastewaters: Simultaneous sorption of Co2+, Cu2+, Ni2+, Pb2+, and Zn2+ ions, J. Environ. Chem. Eng. 3 (2015) 2416–2425.

[41] M. Aziz, S.G. Beheir, Removal of 60Co and 134Cs from radioactive process waste water by flotation, J. Radioanal. Nucl. Chem. 191 (1995) 53–66.

[42] H. Polat, D. Erdogan, Heavy metal removal from waste waters by ion flotation, J. Hazard. Mater. 148 (2007) 267–273.

[43] A. Walcarius, A.M. Lamdaouar, K. El Kacemi, B. Marouf, J. Bessiere, Recovery of lead-loaded zeolite particles by flotation, Langmuir. 17 (2001) 2258–2264.

[44] H. Zhang, Y.K. Kim, T.N. Hunter, A.P. Brown, J.W. Lee, D. Harbottle, Organically modified clay with potassium copper hexacyanoferrate for enhanced Cs+ adsorption capacity and selective recovery by flotation, J. Mater. Chem. A. 5 (2017) 15130–15143.

[45] T. Wajima, Ion Exchange Properties of Japanese Natural Zeolites in Seawater, Anal.

Sci. 29 (2013) 139–141.

[46]   B. Salbu, H.E. Bjørnstad, I. Svaren, S.L. Prosser, R.A. Bulman, B.R. Harvey, M.B. Lovett, Size distribution of radionuclides in nuclear fuel reprocessing liquids after mixing with seawater, Sci. Total Environ. 130 (1993) 51–63.

[47]   M. Chino, H. Nakayama, H. Nagai, H. Terada, G. Katata, H. Yamazawa, Preliminary estimation of release amounts of 131I and 137Cs accidentally discharged from the Fukushima Daiichi nuclear power plant into the atmosphere, J. Nucl. Sci. Technol. 48 (2011) 1129–1134.

[48]   H. Kato, Y. Onda, M. Teramage, Depth distribution of 137 Cs, 134 Cs, and 131 I in soil profile after Fukushima Dai-ichi Nuclear Power Plant accident, J. Environ. Radioact. 111 (2012) 59–64.

[49]   S. Ueda, H. Hasegawa, H. Kakiuchi, N. Akata, Y. Ohtsuka, S. Hisamatsu, Fluvial discharges of radiocaesium from watersheds contaminated by the Fukushima Dai-ichi Nuclear Power Plant accident, Japan, J. Environ. Radioact. 118 (2013) 96–104.

[50]   L.M. Cabezon, M. Caballero, R. Cela, J.A. Perez-Bustamante, Simultaneous separation of copper, cadmium and cobalt from sea-water by co-flotation with octadecylamine and ferric hydroxide as collectors, Talanta. 31 (1984) 597–602.

[51]   S. Cheng, M. Syamsiro, K. Yoshikawa, Effect of HCl Pretreatment on the Performance of Natural Zeolite in a two-stage Pyrolysis and Catalytic Reforming of Polypropylene and Polystyrene, in: 19th Res. Debate, Research Association For Feedstock Recycling of Plastics Japan, Kitakyushu, 2016. http://www.fsrj.org/act/7_nenkai/16-summer/proceeding 16-summer/4.pdf.

[52]   J. Chorover, S. Choi, M.K. Amistadi, K.G. Karthikeyan, G. Crosson, K.T. Mueller, Linking cesium and strontium uptake to kaolinite weathering in simulated tank waste leachate, Environ. Sci. Technol. 37 (2003) 2200–2208.

[53]   Y.S. Ho, G. McKay, Pseudo-second order model for sorption processes, Process Biochem. 34 (1999) 451–465.

[54]   S. Azizian, Kinetic models of sorption: A theoretical analysis, J. Colloid Interface Sci. 276 (2004) 47–52.

[55]   F.-C. Wu, R.-L. Tseng, S.-C. Huang, R.-S. Juang, Characteristics of pseudo-second-order kinetic model for liquid-phase adsorption: A mini-review, Chem. Eng. J. 151 (2009) 1–9.

[56]   T. Shahwan, Sorption kinetics: Obtaining a pseudo-second order rate equation based on a mass balance approach, J. Environ. Chem. Eng. 2 (2014) 1001–1006.

[57]   F.A. Rafiqi, K. Majid, Removal of copper from aqueous solution using polyaniline and polyaniline/ferricyanide composite, J. Environ. Chem. Eng. 3 (2015) 2492–2501.

[58]   N. Gupta, R. Sen, Kinetic and equilibrium modelling of Cu (II) adsorption from aqueous solution by chemically modified Groundnut husk (Arachis hypogaea), J. Environ. Chem. Eng. 5 (2017) 4274–4281.

[59]   J.A. Cotruvo, Water Desalination Processes and Associated Health and Environmental Issues, WC&P Int. (2005). http://www.wcponline.com/2005/01/31/water-desalination-processes-associated-health-environmental-issues/ (accessed December 28, 2017).

[60] A. Charkhi, H. Kazemian, M. Kazemeini, Optimized experimental design for natural clinoptilolite zeolite ball milling to produce nano powders, Powder Technol. 203 (2010) 389–396.

[61] C. Kosanović, B. Subotić, A. Čižmek, Thermal analysis of cation-exchanged zeolites before and after their amorphization by ball milling, Thermochim. Acta. 276 (1996) 91–103.

[62] P.A. Zielinski, A. Van Neste, D.B. Akolekar, S. Kaliaguine, Effect of high-energy ball milling on the structural stability, surface and catalytic properties of small-, medium- and large-pore zeolites, Microporous Mater. 5 (1995) 123–133.

[63] A. Dziedzicka, B. Sulikowski, M. Ruggiero-Mikołajczyk, Catalytic and physicochemical properties of modified natural clinoptilolite, Catal. Today. 259 (2016) 50–58.

[64] A. Günay, E. Arslankaya, I. Tosun, Lead removal from aqueous solution by natural and pretreated clinoptilolite: adsorption equilibrium and kinetics, J. Hazard. Mater. 146 (2007) 362–371.

[65] H. Yuh-Shan, Citation review of Lagergren kinetic rate equation on adsorption reactions, Scientometrics. 59 (2004) 171–177.

[66] Y. Kim, Y.K. Kim, S. Kim, D. Harbottle, J.W. Lee, Nanostructured potassium copper hexacyanoferrate-cellulose hydrogel for selective and rapid cesium adsorption, Chem. Eng. J. (2016).

[67] Y.K. Kim, Y. Kim, S. Kim, D. Harbottle, J.W. Lee, Solvent-assisted synthesis of potassium copper hexacyanoferrate embedded 3D-interconnected porous hydrogel for highly selective and rapid cesium ion removal, J. Environ. Chem. Eng. 5 (2017) 975–986.

[68] H. Mimura, T. Kanno, Distribution and fixation of cesium and strontium in zeolite A and chabazite, J. Nucl. Sci. Technol. 22 (1985) 284–291.

[69] T. Shahwan, D. Akar, A.E. Eroğlu, Physicochemical characterization of the retardation of aqueous Cs + ions by natural kaolinite and clinoptilolite minerals, J. Colloid Interface Sci. 285 (2005) 9–17.

[70] A.M. El-Kamash, Evaluation of zeolite A for the sorptive removal of Cs+ and Sr 2+ ions from aqueous solutions using batch and fixed bed column operations, J. Hazard. Mater. 151 (2008) 432–445.

[71] M.W. Munthali, E. Johan, H. Aono, N. Matsue, Cs+ and Sr2+ adsorption selectivity of zeolites in relation to radioactive decontamination, J. Asian Ceram. Soc. 3 (2015) 245–250.

[72] M.A. Olatunji, M.U. Khandaker, H.N.M.E. Mahmud, Y.M. Amin, Influence of adsorption parameters on cesium uptake from aqueous solutions- a brief review, RSC Adv. (2015) 71658–71683.

[73] B. Ma, S. Oh, W.S. Shin, S.-J. Choi, Removal of Co2+, Sr2+ and Cs+ from aqueous solution by phosphate-modified montmorillonite (PMM), Desalination. 276 (2011) 336–346.

[74] M. Valisko, D. Boda, D. Gillespie, Selective adsorption of ions with different diameter

and valence at highly charged interfaces, J. Phys. Chem. C. 111 (2007) 15575–15585.

[75] B. Ersoy, M.S. Çelik, Electrokinetic properties of clinoptilolite with mono-and multivalent electrolytes, Microporous Mesoporous Mater. 55 (2002) 305–312.

[76] V.J. Inglezakis, The concept of "capacity" in zeolite ion-exchange systems, J. Colloid Interface Sci. 281 (2005) 68–79.

[77] S. Wang, Y. Peng, Natural zeolites as effective adsorbents in water and wastewater treatment, Chem. Eng. J. 156 (2010) 11–24.

[78] A. Jaskūnas, Adsorption of potassium ions on natural zeolite : kinetic and equilibrium studies, 26 (2015) 69–78.

[79] E. Başçetin, G. Atun, Adsorptive removal of strontium by binary mineral mixtures of montmorillonite and zeolite, J. Chem. Eng. Data. 55 (2009) 783–788.

[80] R.D. Rani, P. Sasidhar, Sorption of cesium on clay colloids: kinetic and thermodynamic studies, Aquat. Geochemistry. 18 (2012) 281–296.

[81] M. Endo, E. Yoshikawa, N. Muramatsu, N. Takizawa, T. Kawai, H. Unuma, A. Sasaki, A. Masano, Y. Takeyama, T. Kahara, The removal of cesium ion with natural Itaya zeolite and the ion exchange characteristics, J. Chem. Technol. Biotechnol. 88 (2013) 1597–1602.

[82] S. Coruh, Immobilization of copper flotation waste using red mud and clinoptilolite, Waste Manag. Res. 26 (2008) 409–418.

[83] A.S. Moharir, D. Kunzru, D.N. Saraf, Effect of adsorbent particle size distribution on breakthrough curves for molecular sieve columns, Chem. Eng. Sci. 35 (1980) 1795–1801.

[84] D.R. Kaushal, K. Sato, T. Toyota, K. Funatsu, Y. Tomita, Effect of particle size distribution on pressure drop and concentration profile in pipeline flow of highly concentrated slurry, Int. J. Multiph. Flow. 31 (2005) 809–823.

[85] R.M. Rahman, S. Ata, G.J. Jameson, The effect of flotation variables on the recovery of different particle size fractions in the froth and the pulp, Int. J. Miner. Process. 106 (2012) 70–77.

[86] B. Mikoda, A. Gruszecka-Kosowska, A. Klimek, Copper flotation waste from KGHM as potential sorbent for heavy metal removal from aqueous solutions, Hum. Ecol. Risk Assess. An Int. J. 23 (2017) 1610–1628.

[87] H. Zhang, S. Tangparitkul, B. Hendry, J. Harper, Y.K. Kim, T.N. Hunter, J.W. Lee, D. Harbottle, Selective separation of cesium contaminated clays from pristine clays by flotation, Chem. Eng. J. (2018).

[88] R. Harjula, J. Lehto, Effect of sodium and potassium ions on cesium absorption from nuclear power plant waste solutions on synthetic zeolites, Nucl. Chem. Waste Manag. 6 (1986) 133–137.

[89] G.S., G.Foteini. G.Dionisios, M. Ioannis, Potassium Solution Concentration Effect on Cs Sorption in An Acid Soil, in: Prot. Restor. Environ. XI, Greece, 2012: pp. 740–747.

[90] H. Mimura, Y. Ishihara, K. Akiba, Adsorption behavior of americium on zeolites, J. Nucl. Sci. Technol. 28 (1991) 144–151.
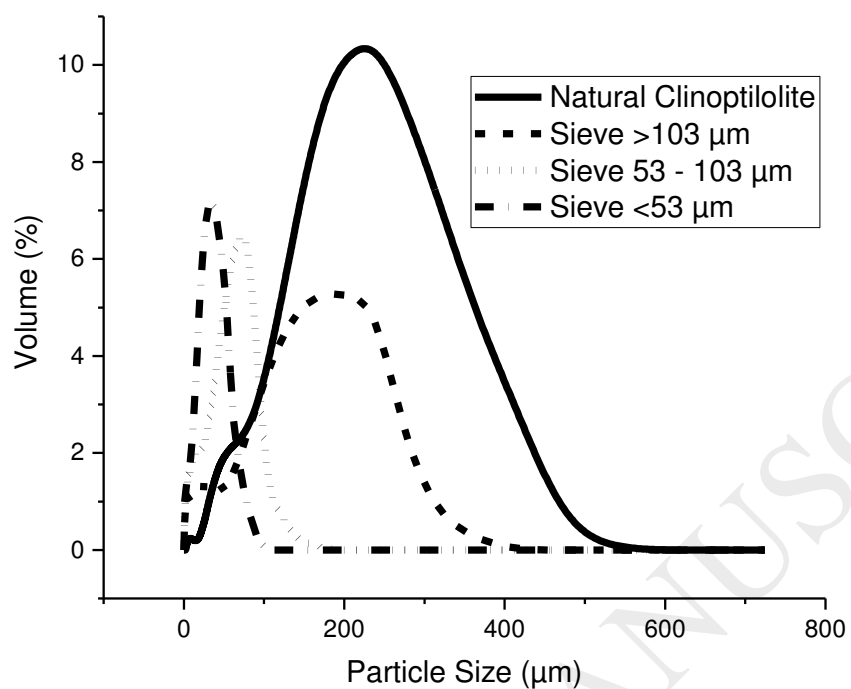
Figure 1: Particle size distributions of natural clinoptilolite for different sieve fractions comminuted using a ball mill.
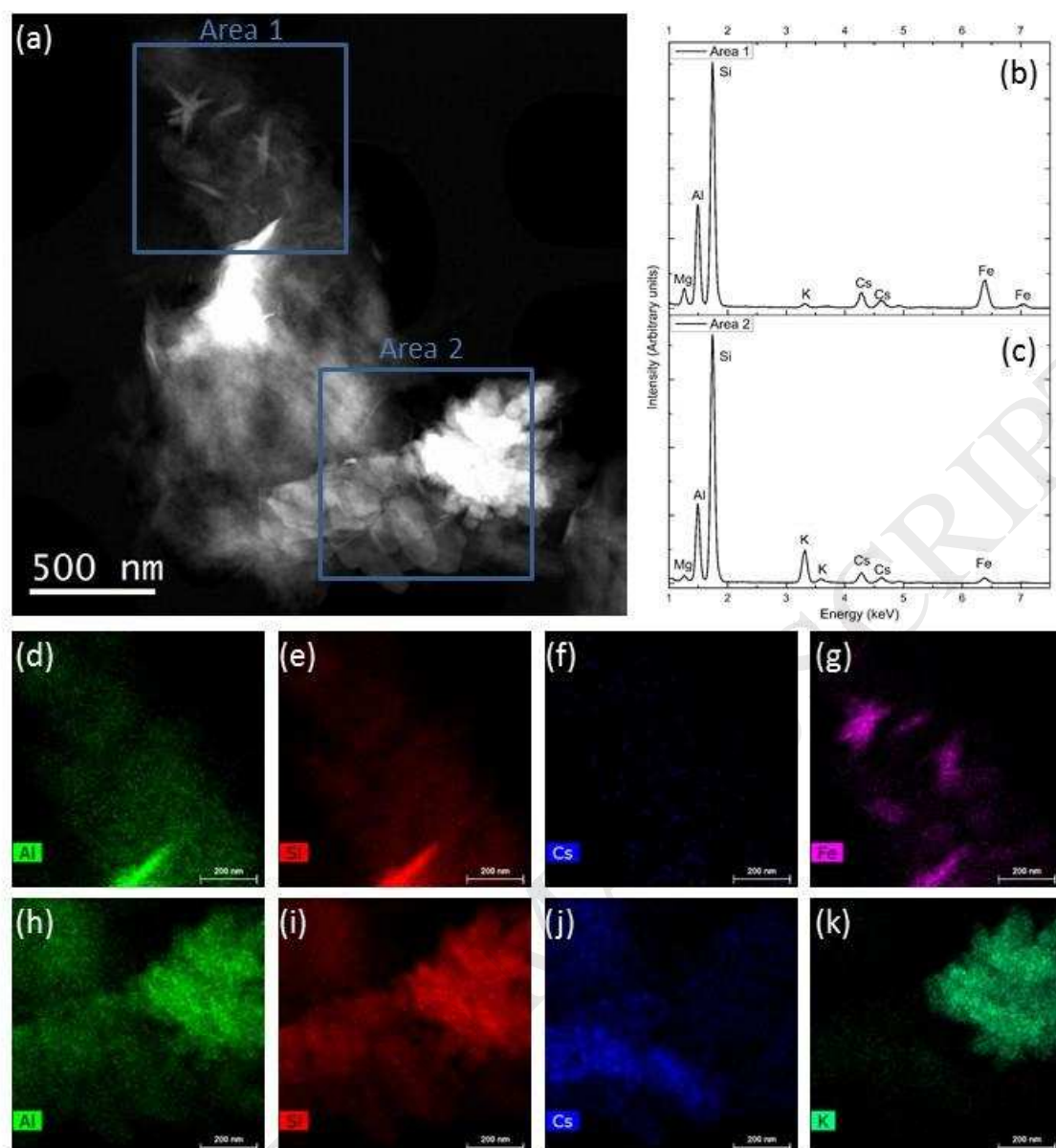
Figure 2: Electron microscopy analysis of natural clinoptilolite after equilibrium adsorption of 5000 ppm cesium chloride. (a) HAADF STEM image of part of the sample, with areas indicated for further analysis. EDX spectra from these two regions are shown in (b) and (c), with the spatial distribution of elements shown for Area 1 in (d) Al, (e) Si, (f) Cs and (g) Fe, and for Area 2 in (h) Al, (i) Si, (j) Cs and (k) K.
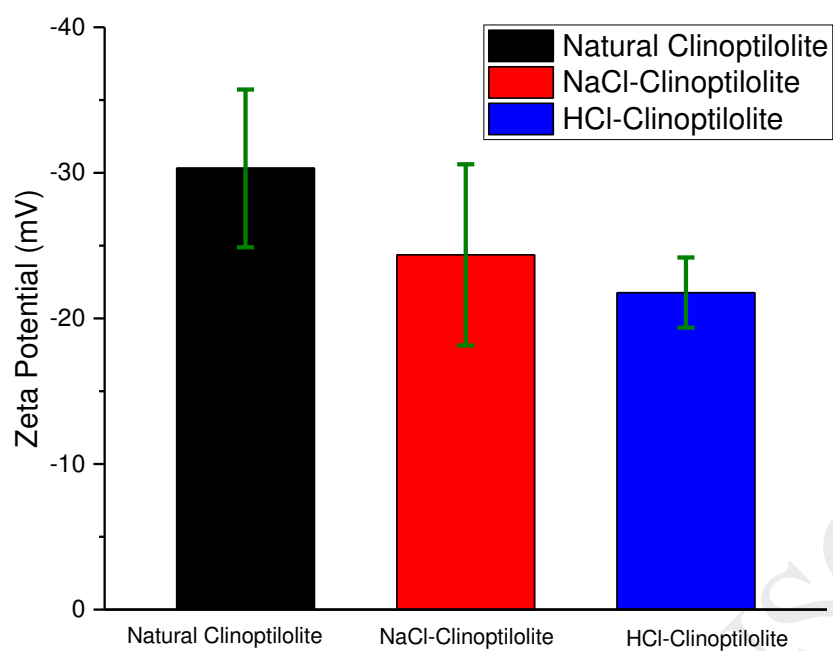
Figure 3: Zeta potential of natural and pre-activated clinoptilolite (HCl-Clinoptilolite and NaCl-Clinoptilolite) at neutral pH.
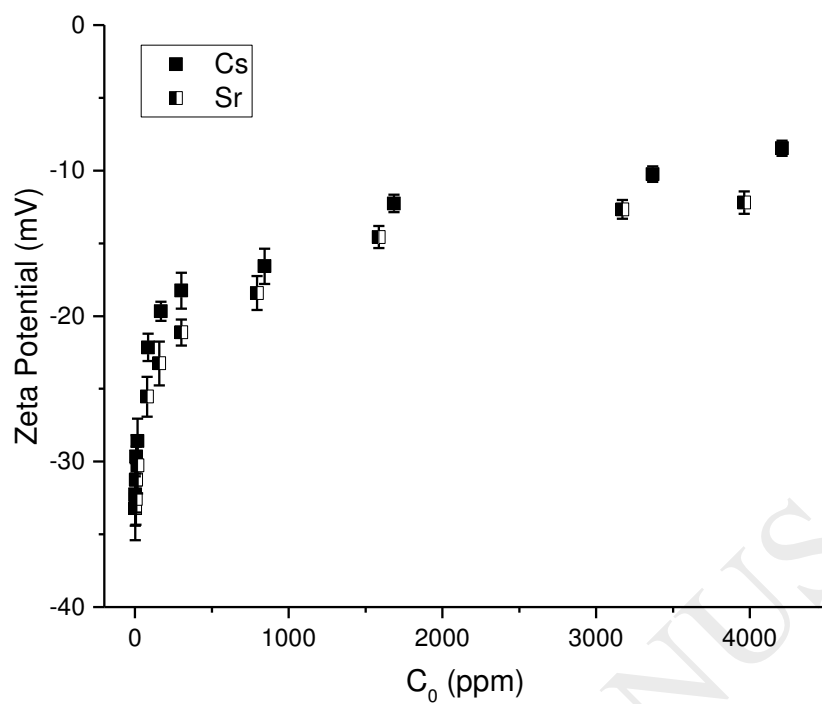
Figure 4: Zeta potential of natural clinoptilolite at neutral pH with different concentrations of Cs^+ and Sr^{2+} ions.
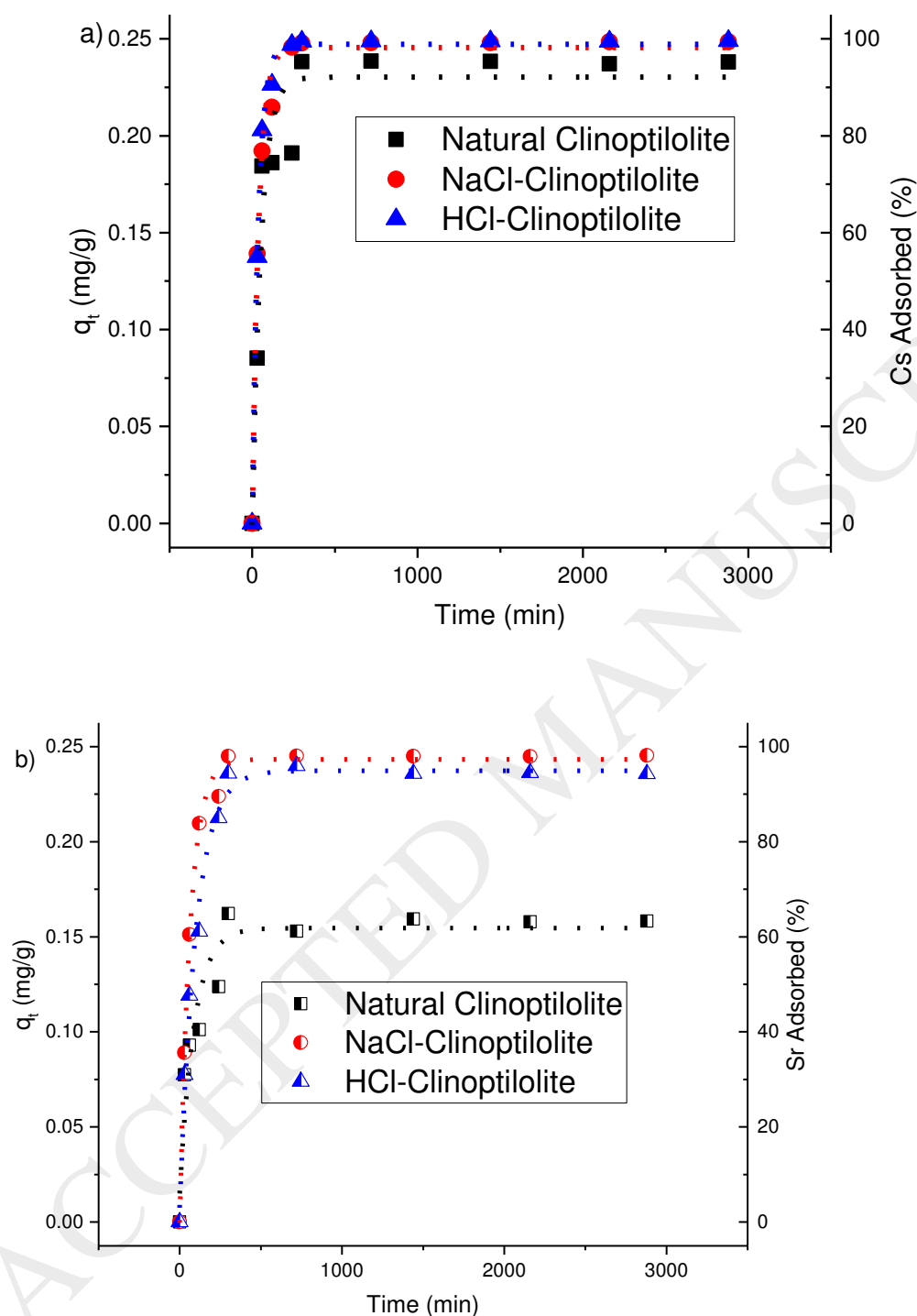
Figure 5: Uptake of 5 ppm cesium and strontium chloride solutions after different adsorption times, from 15 min to 48 h, onto natural and pre-activated clinoptilolite (HCl-Clinoptilolite and NaCl-Clinoptilolite); a) Cs^+ and b) Sr^{2+}. Left vertical axes represent adsorption per mass of ion-exchange, while right vertical represent total removal percentages.
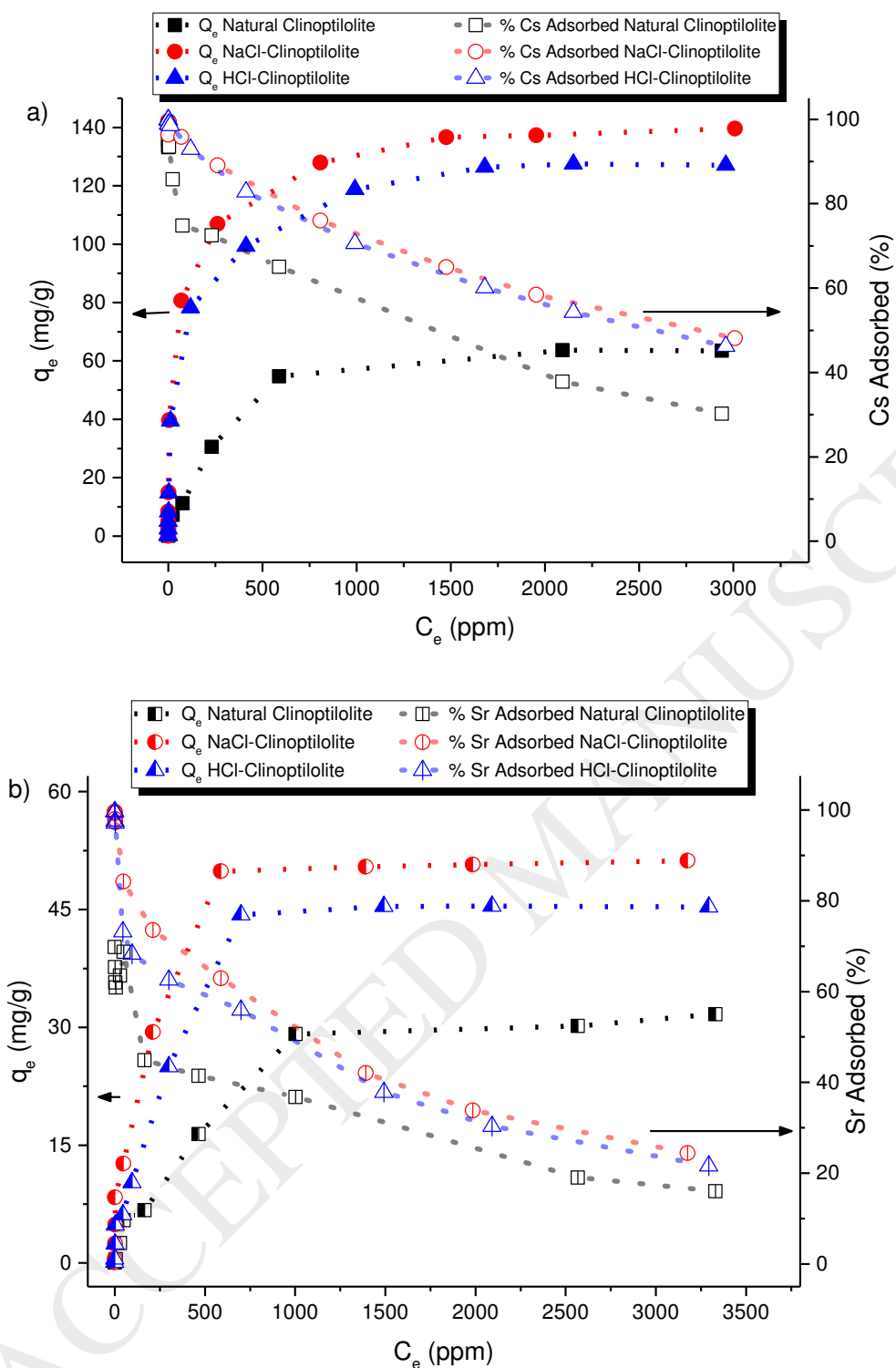
Figure 6: Equilibrium uptake per mass of ion-exchange resin (mg/g) (left, closed symbols) and adsorption percent (right, open symbols) versus cesium and strontium salt concentration onto natural and pre-activated clinoptilolite; a) Cs^+ and b) Sr^{2+}. Connecting dashed lines are to guide the eye.
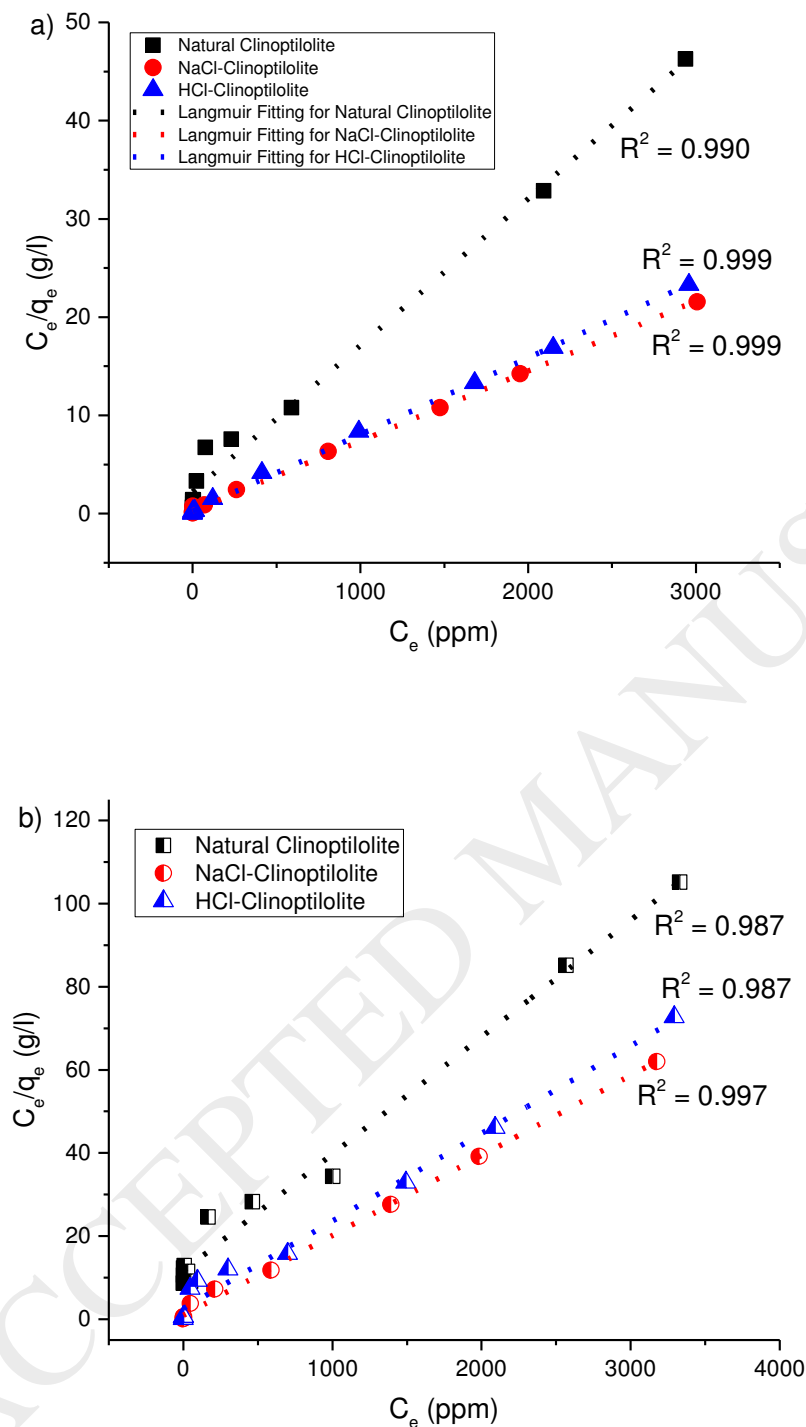
Figure 7: Langmuir isotherms of equilibrium salt adsorption for a) Cs^+ and b) Sr^{2+} onto natural and pre-activated clinoptilolite. Dashed lines represent linear fits.
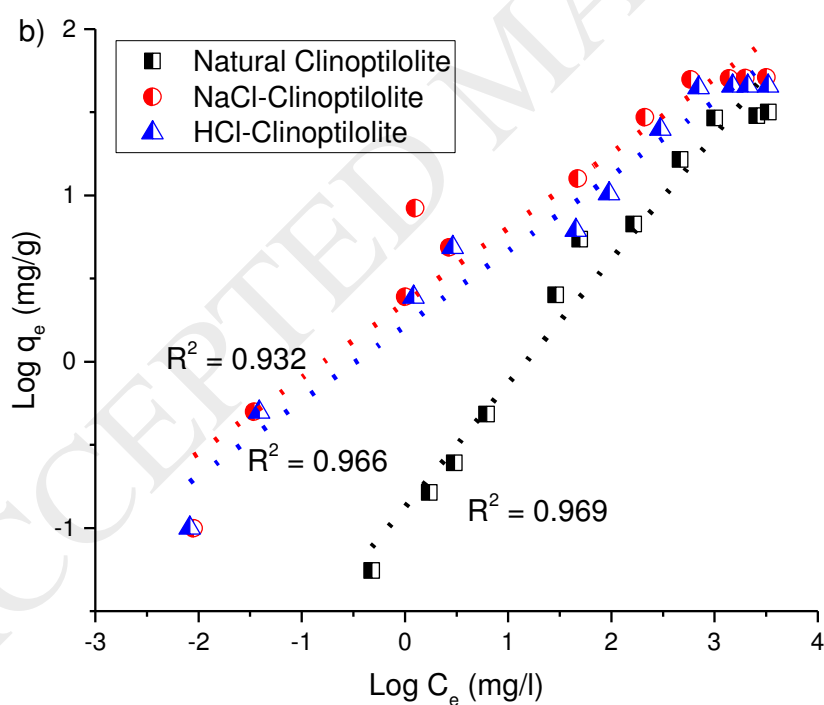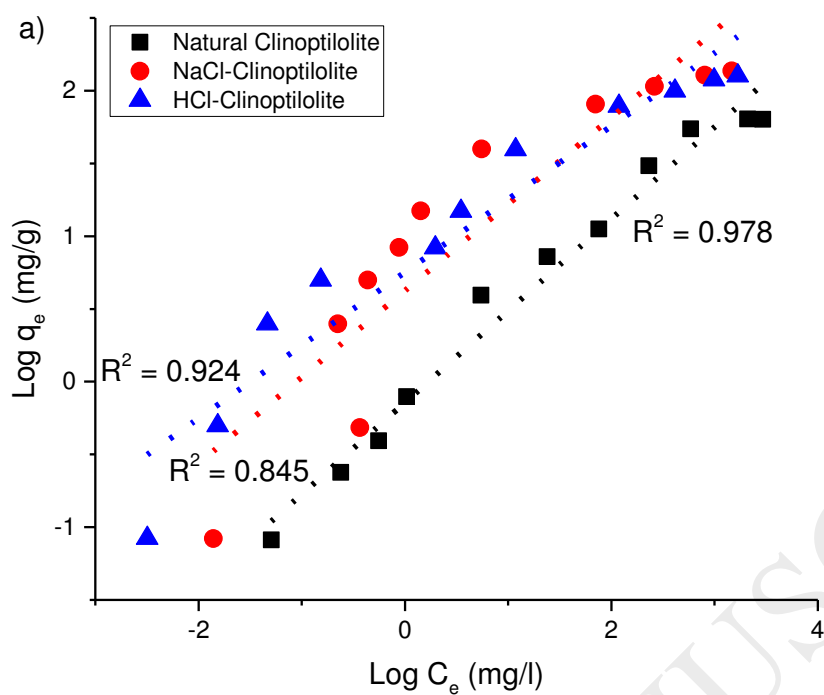
Figure 8: Freundlich isotherms of equilibrium salt adsorption for a) Cs^+ and b) Sr^{2+} onto natural and pre-activated clinoptilolite. Dashed lines represent linear fits.
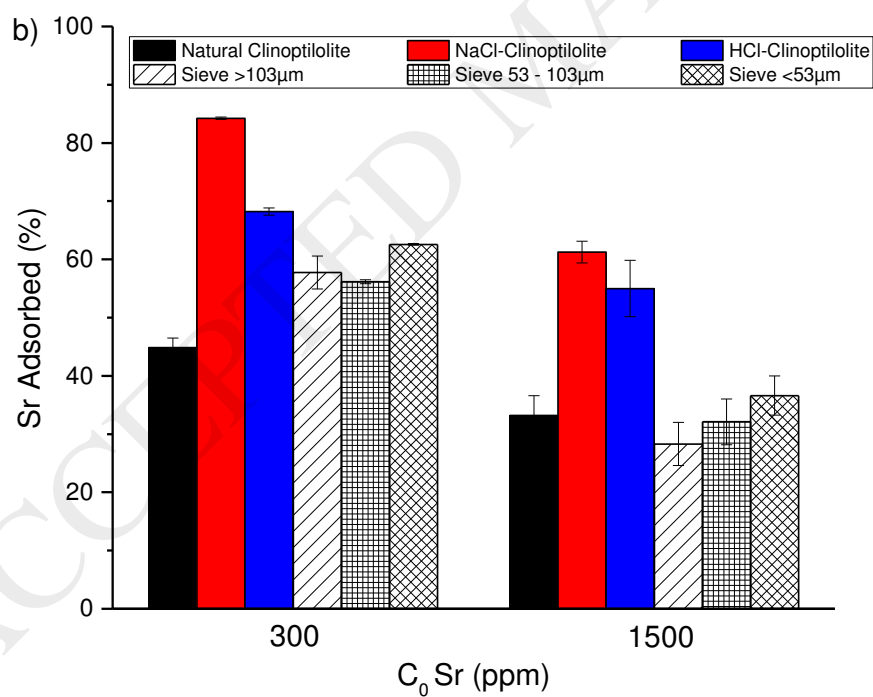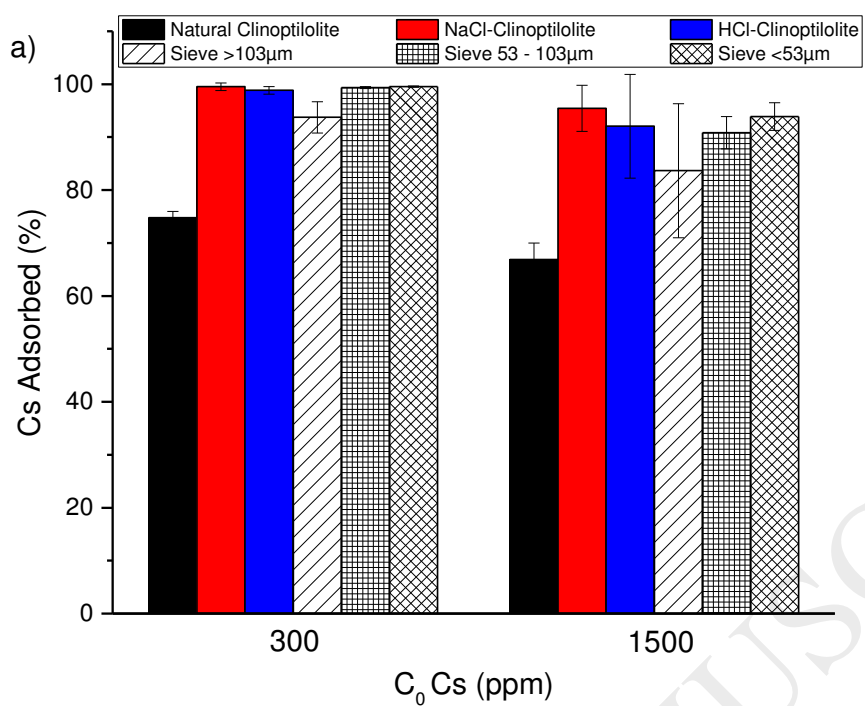
Figure 9: Total adsorption percent for different clinoptilolite treatments (acid and salt activation, as well as three milled fractions) at two different initial salt concentrations, in comparison to the natural mineral; a) Cs^+ and b) Sr^{2+}.
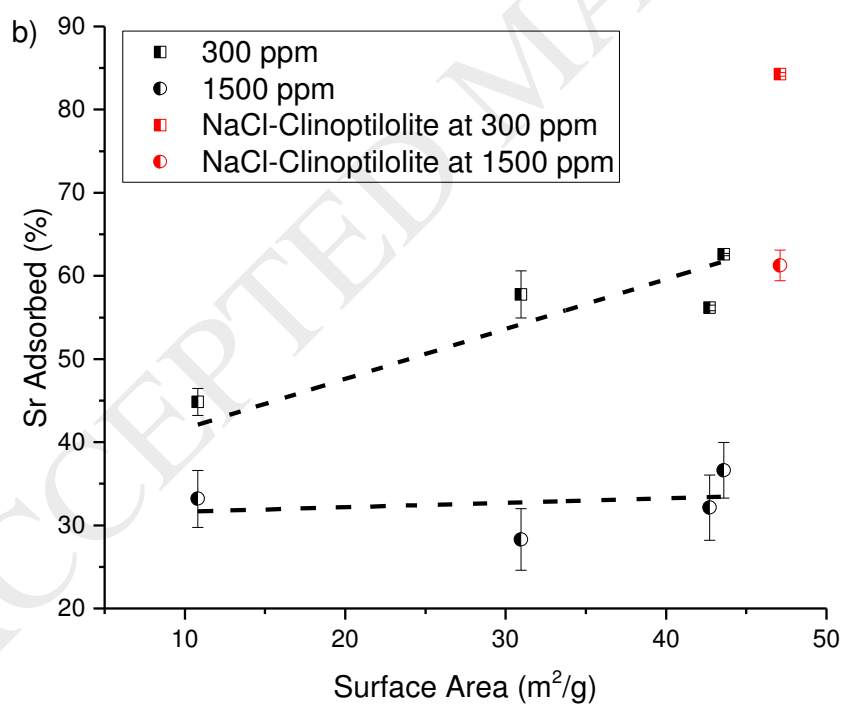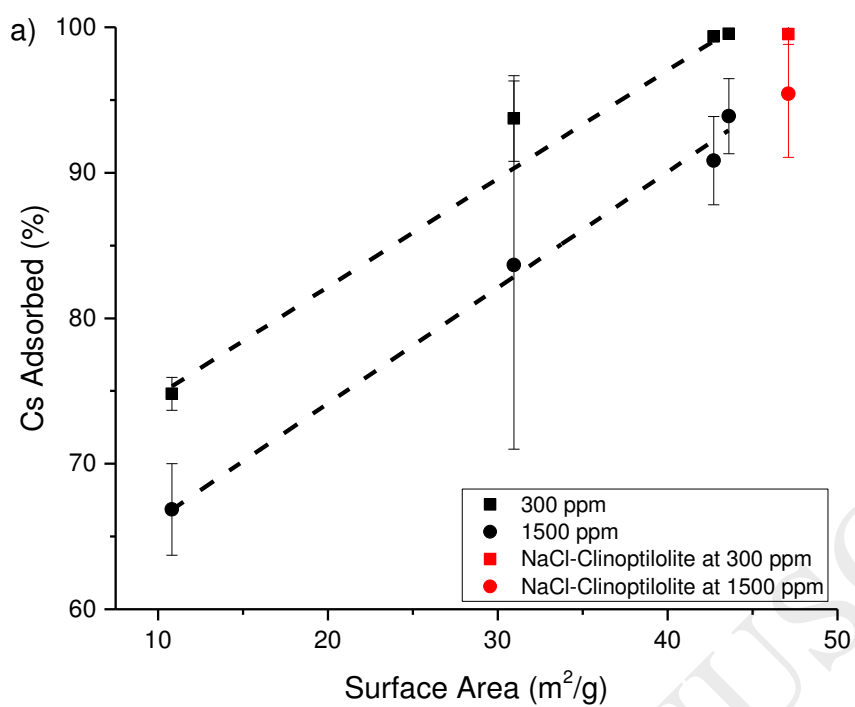
Figure 10: Adsorption percent versus specific surface area for the different mill fractions, as well as salt activated clinoptilolite at two different initial salt concentrations; a) Cs^+ and b) Sr^{2+}. Dashed lines represent linear fits to the milled fractions.
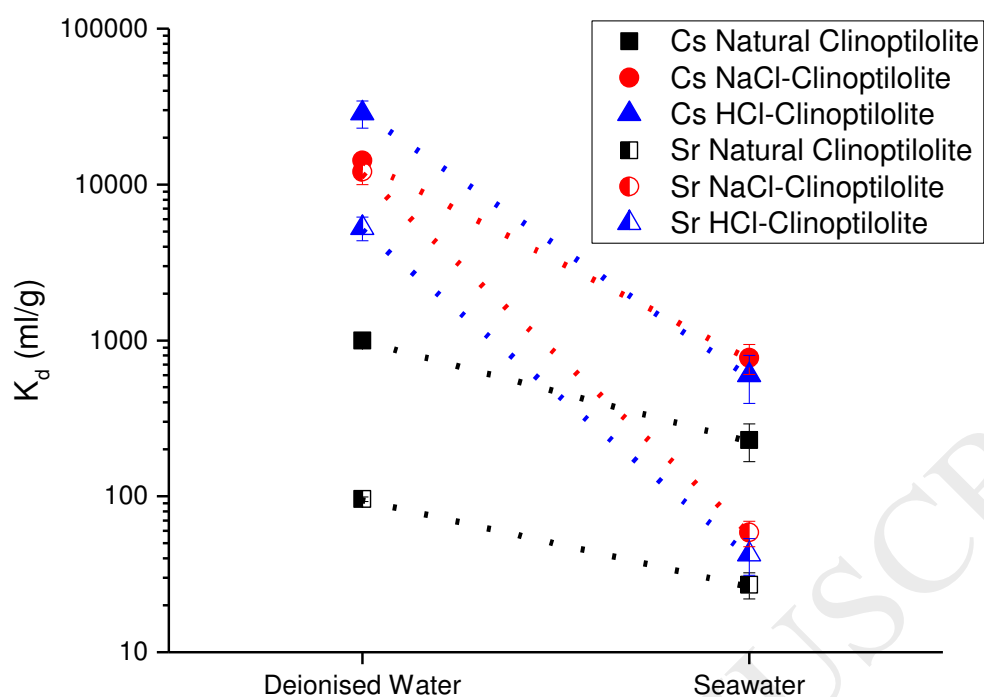
Figure 11: The distribution coefficent (K_d) for 5 ppm Cs^+ and Sr^{2+} solutions in deionised water and in a simulated seawater, with represenative concentrations of K^+ (380 ppm), Na^+ (10556 ppm) and Ca^{2+} (400 ppm). Data shown for natural and pre-activated clinoptilolite.
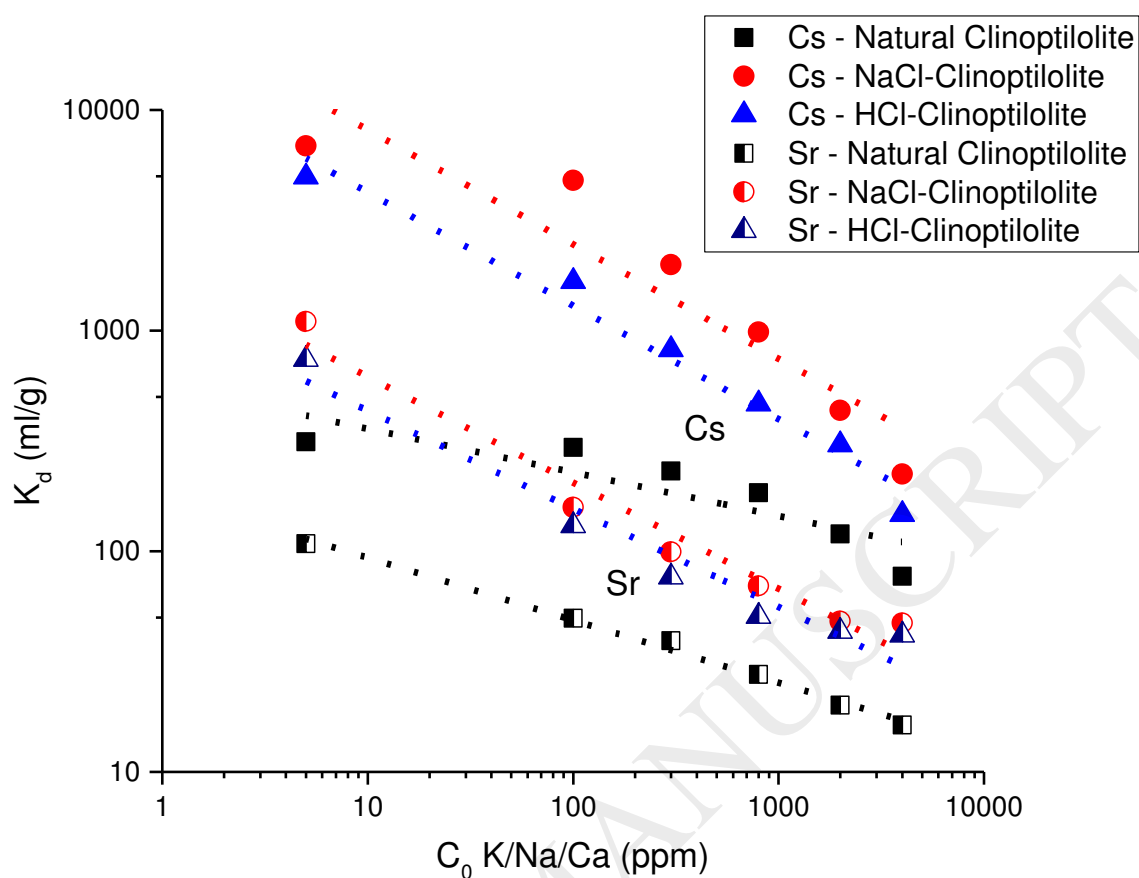
Figure 12: The distribution coefficent (K_d) for 5 ppm of Cs^+ and Sr^{2+} solutions in different concentrations of K^+, Na^+, Ca^{2+} (1:1:1 ratio of each) from 5 to 4000 ppm. Data shown for natural and pre-activated clinoptilolite. Dashed lines represent log-log fits.

Table 1: Pseudo-second order rate constants (k₂), initial adsorption rates (h) and adsorbed solute amounts at equilibrium (qₑ) from dynamic uptake tests of Cs⁺ and Sr²⁺ solutions. Data shown for natural clinoptiloilite at 5 ppm, 300 ppm and 1500 ppm, as well as sodium and acid activated clinoptilolite at 5 ppm.

Cs^+				
Material	k_2	h	$q_{e,cal}$	$q_{e,exp}$
	(g/mg.min)	(mg/g.min)	(mg/g)	(mg/g)
Natural clinoptilolite (5 ppm)	0.163	0.009	0.241	0.238
Natural clinoptilolite (300 ppm)	0.003	0.353	11.532	11.185
Natural clinoptilolite (1500 ppm)	0.001	1.980	61.377	59.365
NaCl activated clinoptilolite (5 ppm)	0.383	0.024	0.250	0.248
HCl activated clinoptilolite (5 ppm)	0.472	0.029	0.250	0.249
Sr^{2+}				
Material	k_2	h	$q_{e,cal}$	$q_{e,exp}$
	(g/mg.min)	(mg/g.min)	(mg/g)	(mg/g)
Natural clinoptilolite (5 ppm)	0.183	0.005	0.161	0.158
Natural clinoptilolite (300 ppm)	0.003	0.142	7.143	6.843
Natural clinoptilolite (1500 ppm)	0.001	0.796	30.615	29.348
NaCl activated clinoptilolite (5 ppm)	0.186	0.011	0.248	0.245
HCl activated clinoptilolite (5 ppm)	0.127	0.007	0.240	0.236

Table 2: Langmuir isotherm fit parameters for equilibrium Cs^+ and Sr^{2+} adsorption on natural clinoptilolite, as well as salt and acid activated clinoptilolite.

Cs^+			
Material	Q_c (mg/g)	b (dm^3/g)	R^2
Natural clinoptilolite	67.046	0.007	0.990
NaCl activated clinoptilolite	140.533	0.030	0.999
HCl activated clinoptilolite	128.167	0.025	0.999
Sr^{2+}			
Material	Q_c (mg/g)	b (dm^3/g)	R^2
Natural clinoptilolite	35.557	0.002	0.987
NaCl activated clinoptilolite	51.975	0.021	0.997
HCl activated clinoptilolite	47.489	0.008	0.987

Table 3: Freundlich isotherm fit parameters for equilibrium Cs^+ and Sr^{2+} adsorption on natural clinoptilolite, as well as salt and acid activated clinoptilolite.

Cs^+			
Material	**K_f (mg/g)**	**n**	**R^2**
Natural clinoptilolite	0.143	1.585	0.978
NaCl activated clinoptilolite	0.615	1.863	0.845
HCl activated clinoptilolite	0.730	2.125	0.924
Sr^{2+}			
Material	**K_f (mg/g)**	**n**	**R^2**
Natural clinoptilolite	0.075	1.342	0.969
NaCl activated clinoptilolite	0.354	2.222	0.932
HCl activated clinoptilolite	0.451	2.218	0.966